# PREDICTION OF GRINDING MACHINABILITY WHEN GRIND ALUMINIUM ALLOY USING WATER BASED ZINC OXIDE NANOCOOLANT

SUGANTHI A/P JAYARAMAN

UNIVERSITI MALAYSIA PAHANG

# PREDICTION OF GRINDING MACHINABILITY WHEN GRIND ALUMINIUM ALLOY USING WATER BASED ZINC OXIDE NANOCOOLANT

SUGANTHI A/P JAYARAMAN

Report submitted in partial fulfilment of the requirements
for the award of Bachelor of Mechanical Engineering with (Manufacturing)

Faculty of Mechanical Engineering
UNIVERSITI MALAYSIA PAHANG

JUNE 2012

## EXAMINER APPROVAL

I certify that the project entitled “Prediction of Grinding Machinability When Grind Aluminium Alloy Using Water Based Zinc Oxide Nanocoolant” is written by Suganthi A/P Jayaraman. I have examined the final copy of this project and in my opinion; it is fully adequate in terms of scope and quality for the award of the degree of Bachelor of Engineering. I herewith recommend that it be accepted in partial fulfilment of the requirements for the degree of Bachelor of Mechanical Engineering with Manufacturing.

Signature :
Name of Panel: MR. NASRUL HADI JOHARI
Position :
Date :

## SUPERVISOR'S DECLARATION

We hereby declare that we have checked this project report and in our opinion this project is satisfactory in terms of scope and quality for the award of the degree of Bachelor of Mechanical Engineering with "specialization".

Signature :
Name of Supervisor : DR.KUMARAN KADIRGAMA
Position :
Date :

## STUDENT'S DECLARATION

I hereby declare that the work in this report is my own except for quotations and summaries which have been duly acknowledged. The report has not been accepted for any degree and is not concurently submitted for award of other degree.

Signature :
Name : SUGANTHI JAYARAMAN
ID Number : ME08059
Date :

**Dedicated to my beloved parents**

**(Mr. Jayaraman & Mrs. Tangeswary)**

## ACKNOWLEDGEMENTS

This accomplishment was not done by me alone. There are a lot of good spirits and angels who guided and motivated me along the way. I would like to take this opportunity to express my heartiest gratitude to all of them.

Firstly I would like thank the almighty for blessing me with all the courage and strength that took to complete my final year project in time without much predicament. The next credit goes to my parents Mr.Jayaraman and Mrs.Tangeswary and also my beloved siblings for their endless encouragement and great support throughout this period of one year.

I am grateful and would like to express my sincere gratitude to my supervisor Dr.Kumaran Kadirgama for her germinal ideas, invaluable guidance, continuous encouragement and constant support in making this research possible. My sincere appreciation also goes to En. Wan Azmi for his relentless guidance when preparing nanocoolant for this project.

My sincere thanks go to all my labmates and members of the staff of the Mechanical Engineering Department, UMP, who helped me in many ways and made my stay at UMP pleasant and unforgettable.

I hope this research project will be helpful for those who need reference in the field of metal casting process. Finally I would like to express my gratefulness to all of them who involved directly or indirectly in the completion of my final year project and thesis. Thank you.

## ABSTRACT

This thesis deals with the prediction of grinding machinability when grind aluminium alloy using water based zinc oxide nanocoolant. The objective of this thesis is to find the optimum parameter which was the depth of cut, investigate the surface roughness and wear produced during experimental and develop the prediction model with the usage of Artificial Neural Network (ANN). The work piece used was aluminium alloy and zinc oxide nanocoolant as the grinding coolant. The grinding process was carried out with the usage of silicon carbide as the grinding wheel. The design of experiment was nine experiments for each single and multi-pass. The parameter used in this study was various depth of cut. The thesis describes the effect of coolant on the surface roughness and also the wheel wear. As a result, the usage of nanocoolant lead to the decrease in the surface roughness and also the wheel wear. The 2D microstructure of the grinded material was observed to view the material condition for various depth of cut. The surface roughness for grinding process using nanocoolant has a better result compared to water based coolant. Next, the result was trained using ANN to develop the prediction model for various depth of cut. Basically, the surface roughness became constant at one point with the increasing of depth of cut, whereby plastic deformation occurs. To conclude this study, the objective of the study was achieved, 1) the optimum depth of cut was 5μm, 2) the surface roughness of the material was investigated, whereby the roughness increase with the increasing of depth of cut and 3) the prediction model was done with ANN. As for the recommendation, the usage of different type of nanocoolant with various concentration and different particle sizes may affect the surface roughness of the material and also the wear produced. Next, the usage of different type and size of wheel should be considered in order to obtain a better surface finish.

# ABSTRAK

Tesis ini membentangkan ramalan pengisaran di mesin apabila mengisar aloi aluminium menggunakan zink oksida nanocoolant berasaskan air. Objektif tesis ini a dalah untuk mencari parameter kedalaman potongan yang optimum, menyiasat kekasaran permukaan dan kehausan roda yang dihasilkan semasa eksperimen dan membangunkan model ramalan dengan penggunaan Artificial Neural Network (ANN ). Bahan kerja yang digunakan adalah aloi aluminium dan cecair penyejuk nano zink oksida sebagai penyejuk pengisaran. Proses pengisaran dijalankan dengan peng gunaan silikon karbida sebagai roda pengisaran. Reka bentuk eksperimen adalah sembilan eksperimen bagi setiap laluan tunggal dan pelbagai. Parameter yang digunakan dalam kajian ini adalah pelbagai kedalaman potongan. Tesis ini menerangkan kesan penyejuk pada kekasaran permukaan dan juga kehausan roda. Hasilnya, penggunaan cecair penyejuk nano membawa kepada penurunan dalam kekasaran permukaan dan juga kehausan roda. 2D Mikrostruktur terhadap bahan yang dikisar diperhatikan untuk mengkaji keadaan bahan bagi pelbagai kedalaman potongan. Kekasaran permukaan untuk proses menggisar menggunakan cecair penyejuk nano mempunyai hasil yang lebih baik berbanding penyejuk berasaskan air. Seterusnya, keputusan telah dilatih menggunakan ANN untuk membangunkan model ramalan untuk pelbagai kedalaman potongan. Pada asasnya, kekasaran permukaan menjadi malar pada satu titik dengan peningkatan kedalaman potongan, di mana ubah bentuk plastik berlaku. Sebagai kesimpulan kajian ini, objektif kajian telah dicapai, 1) kedalaman optimum potongan adalah 5μm, 2) kekasaran permukaan bahan yang telah disiasat, di mana kekasaran permukaan bahan meningkat dengan peningkatan kedalaman pemotongan dan 3) ramalan model bagi pelbagai kedalaman potongan dicapai dengan ANN. Sebagai cadangan, penggunaan cecair penyejuk nano yang berlainan jenis dengan kepekatan yang pelbagai dan saiz zarah yang berlainan mungkin memberi kesan kekasaran permukaan bahan dan juga kehausan roda yang dihasilkan. Seterusnya, penggunaan roda pengisaran yang

berlainan jenis dan saiz perlu dipertimbangkan untuk mendapatkan kemasan permukaan yang lebih baik.

## TABLE OF CONTENTS

## LIST OF TABLES

## LIST OF FIGURES

## LIST OF SYMBOLS

| | |
|---|---|
| $k_{nf}$ | Thermal conductivity of nanoparticle |
| $k_w$ | Thermal conductivity of water |
| $Cp$ | Heat capacity |
| $Ra$ | Roughness average |
| $Rz$ | Arithmetic mean |
| $Rq$ | Root-mean-square average |
| $T_{nf}$ | Nanoparticle temperature |
| $d_p$ | Nanoparticle diameter |
| $\rho_w$ | Density of water |
| $\rho_{nf}$ | Density of nanoparticle |
| $C_w$ | Specific heat of water |
| $\mu_w$ | Viscosity of water |
| $\mu_{nf}$ | Viscosity of nanoparticle |
| $\omega$ | Weight percent |
| $\phi$ | Volume percent |
| $q$ | Constant heat rate |

## LIST OF ABBREVIATIONS

| | |
|---|---|
| AA | Aluminium Alloy |
| Al | Aluminium |
| ZnO | Zinc Oxide |
| $Al_2O_3$ | Aluminium Oxide |
| $TiO_2$ | Titanium Oxide |
| CuO | Copper Oxide |
| SiC | Silicon Carbide |
| Cr | Chromium |
| Cu | Copper |
| Fe | Ferum |
| Mg | Magnesium |
| Mn | Manganese |
| Si | Silicon |
| Ti | Titanium |
| Zn | Zinc |
| ANN | Artificial Neural Network |
| RMS | Root-Mean-Square |
| AD | Average Deviation |
| SD | Standard Deviation |
| VLD | Validation |
| TRN | Training |

| | |
|---|---|
| TST | Testing |

# CHAPTER 1

# INTRODUCTION

## 1.1 BACKGROUND

Grinding is a precision machining process which is widely used in the manufacture of components requiring fine tolerances and smooth finishes. This research studied the prediction of grinding machinability when grind aluminium alloy using water based zinc oxide nanocoolant. Cutting fluids are used in grinding for a variety of reasons such as improving wheel life, reducing work piece thermal deformation, improving surface finish and flushing away chips. Large fluid delivery and cooling systems are evident in production plants.

High rates of manufactured items have been machined by grinding at some stage of their production process, or have been processed by machines whose precision is a direct result of abrasive operations. However, even being the grinding process the most used in industry for obtaining high level of surface quality, it remains as one of the most difficult and least understood processes (Eastman et al., 2001). That maybe has origin in the mistaken faith the process is extremely complex to be understood due to the large number of cutting edges and irregular geometry, high cutting speed, and very small depth of cut which varies from grain to grain.

Nanocoolant is a new class of fluids engineered by dispersing nanometer-size solid particles in base fluids to increase heat transfer and tribological properties. The

thermal conductivity and the convection heat transfer coefficient of the fluid can be largely enhanced by the suspended nanoparticles (Bin Shen, 2008). Coolants with nanoparticle additives exhibit improved load-carrying capacity, anti-wear and friction reduction properties. These features make the nanocoolant very attractive in some cooling and/or lubricating application in many industries including manufacturing, transportation, energy, and electronics.

## 1.2 PROBLEM STATEMENT

Grinding is recognized as one of the most environmentally unfriendly manufacturing processes. An extensive amount of mist is generated during grinding, and the problem is exacerbated by the use of high wheel speeds. The mist generation rate in grinding is often an order of magnitude higher than that in turning. Millions of workers are engaged in daily manufacturing operations worldwide. However, the health hazards to machine operators and other nearby workers who breathe in this hazardous mist are often overlooked. As environmental regulations get stricter, the cost of disposal or recycling continues to go up. The need for cost-reduction has all promoted the development of new environmentally conscious machining processes.

Cutting fluids are a critical factor in controlling these undesirable effects of elevated temperatures, thermal damage, and dimensional inaccuracies (Khettabi et al., 2010). Cutting fluid reduces the machining power and the associated heat generation, while also enhancing surface quality and reducing wheel wear. Cooling by the fluid removes heat from the tool and the work piece. As an alternative, the recent development of nanocoolants replaced cutting fluids which can be used in grinding. The nanocoolants properties of advanced heat transfer, thermal conductivity and viscosity can provide better cooling and lubricating in the grinding process, and make it production-feasible. The suitable depth of cut is also needs because it can affect the surface texture been rougher and the surface is not shining. When the depth of cut increase, the surface roughness also increase. The results of experiment must consider in different perspective of parameter to get accurate results.

## 1.3 OBJECTIVES

The objectives of this project are:

(i) To find an optimum parameter (depth of cut - to produce better surface roughness and wheel wear).

(ii) To investigate surface roughness and wear produced during experimental.

(iii) To develop Mathematical model to predict surface roughness using Artificial Neural Network (ANN).

## 1.4 SCOPES OF THE PROJECT

The scopes of the project are:

a) Use surface grinding machine for grinding process and conventional abrasive (silicon carbide) as a grinding wheel.

b) Use zinc oxide nanocoolant as cutting fluid for grinding process.

c) Use Perthometer to measure surface roughness.

d) Use tachometer to set the work speed constant which was 200 rpm.

e) Use optical measurement to observe microstructure of material.

f) Number of experiments are 18

g) Parameters for the grinding :

   i) Depth of cut, in the range of (5, 7, 9, 11, 13, 15, 17, 19, 21) µm.

## 1.5 THESIS OUTLINES

Chapter 1 of this thesis is about the background of the grinding process and also nanocoolant. Then it includes the problem caused in grinding process and objective concerning about the investigation of grinding machinability when grind aluminium alloy using water based zinc oxide nanofluid for certain parameters. The scope of this project is to develop a prediction model for surface roughness and wheel wear.

Chapter 2 presents literature review that will focus on recent studies or research by authors related to the grinding machinability when nanocoolant was used as cutting fluid. The formation and characterization of nanocoolant are also discussed here. The literature review can be approximately close to the titles of the project also. From this chapter, the author will get more knowledge on the results of the previous researches and can predict the result for the project.

Chapter 3 is the overview of the preparation of the nanocoolant and experimental work of grinding using conventional abrasive wheel to grind aluminium alloy with zinc oxide nanocoolant. Water based nanocoolant were employed in grinding and the performance was evaluated in terms of surface roughness and wheel wear.

Chapter 4 focuses on the outcomes of the research and discussion. Use perthometer to measure surface roughness. The result need to compare for the grinding process use water based coolant and varies nanocoolant. The model was developed to understand the better machinability in grinding.

Chapter 5 focuses on the conclusions of the project and recommendations for future work. This chapter also will summarize both the results and objectives of the project.

# CHAPTER 2

# LITERATURE REVIEW

## 2.1 INTRODUCTION

In this chapter, it basically describes more about the studies on water based grinding and nanocoolants grinding processes which has been done earlier by other researchers. It also discussed about the aluminium alloy and zinc oxide nanocoolant which has been used in this experiment.

## 2.2 ALUMINIUM ALLOY

Aluminium alloy 6061 is one of the most extensively used of the 6000 series aluminium alloys. It is a versatile heat treatable extruded alloy with medium to high strength capabilities. Based on (V. Songmene et al., 2009) studies, aluminum alloys are among the most commonly used lightweight metallic materials as they offer a number of different interesting mechanical and thermal properties. In addition, they are relatively easy to shape metals, especially in material removal processes, such as machining. In fact, aluminum alloys as a class are considered as the family of materials offering the highest levels of machinability, as compared to other families of lightweight metals such as titanium and magnesium alloys. This machinability quantifies the machining performance, and may be defined for a specific application

by various criteria, such as tool life, surface finish, material removal rate and machine-tool power.

### 2.2.1 Aluminium Alloy Properties

It has been shown that chemical composition (Table 2.1) and physical properties (Table 2.2), structural defects and alloying elements significantly influence machinability (Y. W. Tham et al., 2007). The typical properties of aluminium alloy 6061 include the medium to high strength, good surface finish, good corrosion resistance to sea water and atmospheric conditions, good weldability and brazability, also can be anodized.

**Table 2.1:** Composition in wt% of Aluminium-6061 Alloy

| **Composition (weight %)** | | | | | | | | |
|---|---|---|---|---|---|---|---|---|
| **Al** | **Cr** | **Cu** | **Fe** | **Mg** | **Mn** | **Si** | **Ti** | **Zn** |
| 95.8 - 98.6 | 0.04 - 0.35 | 0.15 - 0.04 | Max 0.7 | 0.8 - 1.2 | Max 0.15 | 0.4 - 0.8 | Max 0.15 | Max 0.25 |

Source: Y. W. Tham et al., 2007

**Table 2.2:** Physical Properties of AA6061

| **Material** | **Density ($kg/m^3$)** | **Melting temperature (°c)** | **Vicker's microhardness (HV)** | **Heat capacity Cp ($Jmol^{-1}$)** | **Ultimate tensile strength(MPa)** |
|---|---|---|---|---|---|
| **AA6061** | 2680 | 582 | 77 | 24.28 | 283 |

Source: Y. W. Tham et al., 2007

### 2.2.2 Application of Aluminium Alloy

Aluminium alloys 6061 are used in many applications due to their wide range of excellent properties. The important factors in selecting aluminium (Al) and its alloys are their high strength-to-weight ratio, their resistance to corrosion by many chemicals, their high thermal and electrical conductivity, high ductility, their non-toxicity, reflectivity, and appearance, and their ease of formability and of machinability. Consequently many properties are of importance in each individual application and the alloy development must focus on maximizing one or a combination of properties at the same time as minimum requirements are fulfilled for the others. The principal uses of aluminium and its alloys, in decreasing order of consumption, are in container and packaging (aluminium cans and foil), in building and other types of construction, in transportation (aircraft and aerospace application, buses, automobiles, rail-road cars, an marine craft), in electrical applications (economical and nonmagnetic electrical conductor), in consumer durables (appliances, cooking utensils, and furniture), and in portable tools. Nearly all high voltage transmission wiring is made of aluminium (R. Khettabi et al., 2010).

## 2.3 GRINDING PROCESS

Grinding is a process carried out with a grinding wheel made up of abrasive grains for removing very fine quantities of material from the work piece surface (Alexius 2008). Low material removal best described for grinding features. The purpose of grinding is to lessen the depth of deformed metal to the point where the last leftovers of damage can be removed by sequence of polishing steps. The scratch depth and the depth of cold worked metal underneath the scratches decrease with decreasing particle have explained the decrease in grinding force as the wheel speed increases as being more due to the favourable kinematic conditions.

Based on (Guhring, 1990) studies, the beneficial effect of more favourable kinematic conditions, and also demonstrates that reduced mechanical strength at elevated temperatures has a critical influence reduction in the grinding tangential force drops with increasing wheel speed and a constant depth of cut. In this case the

explanation does not lie in any reduction in the cross section of the chip, as the depth of cut in the groove remains constant. Higher wheel speeds also result in a less ductile behaviour of the material as it is deformed, and so reduce the force and energy input required for the grinding operation.

Machining with grinding wheels is a very complex process affected by so many factors that a reproducible result is rarely obtained. The most important one is that the cutting ability of the grinding wheel changes considerably during the grinding time. In practice, the grinding process is carried out with cutting parameters which are safe but not optimal. The result of a grinding process can be subdivided into characteristics concerning the geometry and surface integrity of a ground component. The geometrical quantities are dimension, shape and waviness, as essential macro-geometric quantities; whereas the roughness condition is the main micro-geometric quantity. The surface integrity state can be described by residual stresses, hardness and structure of the material (Aguiar et al., 2008).

## 2.4 GRINDING PARAMETER

Grinding is an essential process for final machining of components requiring smooth surfaces and precise tolerances. As compared with other machining processes, grindings costly operation that should be utilized under optimal conditions. Although widely used in industry, grinding remains perhaps the least understood of all machining processes (Rusydah, 2008). The major operating input parameters that influence the output responses, metal removal rate, surface roughness, surface damage, and tool wear, are:

(i) Wheel parameters: abrasives, grain size, grade, structure, binder, shape and dimension.
(ii) Work piece parameters: fracture mode, mechanical properties and chemical composition.
(iii) Process parameters: work speed, depth of cut, feed rate, dressing condition
(iv) Machine parameters: static and dynamic characteristics, spindle system, and table system, etc.

### 2.4.1 Work piece Material

In this project, the material of work piece used was aluminium alloy. This material is one of the parameters that important which influence the surface roughness in grinding process. The material composition is important in effecting the result of the experiment. It is depends on the chemical composition (Table 2.1) and physical properties in (Table 2.2). Aluminium alloys are alloys in which aluminium (Al) is the predominant metal. Aluminium alloy surfaces will keep their apparent shine in a dry environment due to the formation of a clear, protective layer of aluminium oxide.

### 2.4.2 Depth of Cut

The second parameter considered in this experimental study is the depth of cut of the work piece during the machining. Depth of cut is a depth of work material removed per revolution or table pass (Rusydah, 2008). Depth of cut is the thickness of material removed in a machining operation as show in Figure 2.2. This studies lead to formulation of factorial design to predict surface roughness with a power form equation using operation-cutting parameters. Decrease of depth of cut improves surface finish (Thomas, 1997). While (Marinescu, 2001), that focused on studying tool vibration, found that increase of depth of cut improves surface roughness under specific operating conditions.

### 2.4.3 Grinding Wheel

A grinding wheel is an expendable wheel that is composed of an abrasive compound used for various grinding abrasive cutting and abrasive machining operations. They are used in grinding machines. The wheels are generally made from a matrix of coarse particles pressed and bonded together to form a solid, circular shape, various profiles and cross sections are available depending on the intended usage for the wheel (Chris, 2007). They may also be made from a solid steel or aluminium disc with particles bonded to the surface. The manufacture of these wheels is a precise and tightly controlled process, due not only to the inherent safety

risks of a spinning disc, but also the composition and uniformity required to prevent that disc from exploding due to the high stresses produced on rotation. The function of the grinding wheel that clamped to the grinding machine are to remove material from a work piece in an abrasive action**,** each grain acts as a cutting tool**,** and it is a chip formation process.

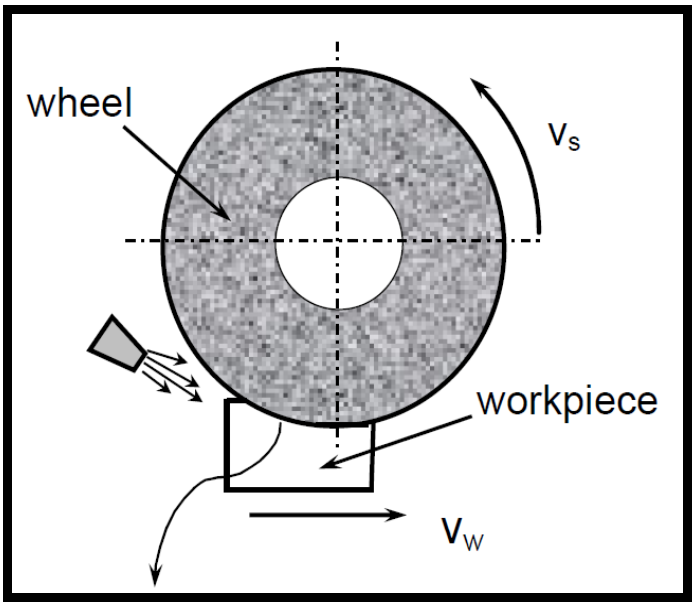


**Figure 2.1 :** Illustration of Grinding Wheel

Source: Chris. 2007

Silicon carbide is the only chemical compound of carbon and silicon. It was originally produced by a high temperature electro-chemical reaction of sand and carbon. Silicon carbide is an excellent abrasive and has been produced and made into grinding wheels and other abrasive products for over one hundred years. Today the material has been developed into a high quality technical grade ceramic with very good mechanical properties. It is used in abrasives, refractories, ceramics, and numerous high-performance applications. The material can also be made an electrical conductor and has applications in resistance heating, flame igniters and electronic components. Structural and wear applications are constantly developing. The properties of silicon carbide are as in (Table 2.3). The silicon carbide wheel has low

density, high strength, low thermal expansion, high thermal conductivity, high hardness, high elastic modulus, and excellent thermal shock resistance.

**Table 2.3:** Mechanical Properties of Silicon Carbide

| Density | Poisson's Ratio | Hardness | Thermal Conductivity |
|---|---|---|---|
| 3.1 gm/cc | 0.14 | 2800 Kg/mm$^2$ | 120 W/m•°K |

## 2.5 HEAT TRANSFER IN GRINDING

The grinding process generates an extremely high input of energy per unit volume of material removed. Virtually all this energy is converted to heat, which can cause high temperatures and thermal damage to the work piece such as work piece burn, phase transformations, undesirable residual tensile stresses, cracks, reduced fatigue strength, and thermal distortion and inaccuracies (Bin Shen, 2008).

Temperatures generated during grinding are a direct consequence of the energy input to the process. In general, the energy or power consumption is an uncontrolled output of the grinding process, which may vary considerably and is sensitive to the wheel condition. Consequently, the temperature generated is also uncontrolled and varying. In-process monitoring of the grinding power, when coupled with a thermal analysis of the grinding process, offers a better approach for estimating grinding temperatures and controlling thermal damage.

According to (Xiang, et al., 2006), thermal analyses of grinding processes are usually based upon the application of moving heat source theory to the work piece being ground. For this purpose, the grinding zone is usually modelled as a band source of heat which moves along the surface of the work piece. All the grinding energy expended in considered to be converted to heat at the grinding zone where the wheel interacts with the work piece. A critical parameter needed for calculating the

temperature responses is the energy partition to the work piece, which is the fraction of the total grinding energy transported to the work piece as heat at the grinding zone. The energy partition depends on the type of grinding, the wheel and work piece materials, and the operating conditions.

## 2.6 INTRODUCTION TO SURFACE ROUGHNESS

A surface defined by ANSI as the boundary that separates an object from the surrounding medium. (Mainsah, 2001) stated in his research that feed, nose radius, work material, speed and angle of turning machine has a significant impact on the surface roughness. The Roughness or rugosity is a measurement of the small-scale variations in the height of a physical surface. This is in contrast to large-scale variations, which may be either part of the geometry of the surface or unwanted 'waviness'. Roughness is sometimes an undesirable property, as it may cause friction, wear, drag and fatigue, but it is sometimes beneficial, as its texture allows surfaces to trap lubricants and prevents them from welding together. It is measuring in different ways for different purposes. While, surface roughness defined as the measurement of the finer surface irregularities in the surface texture (Engineredge, 2007). Surface roughness, Ra rated in arithmetic average deviation of the surface valleys and peaks expressed in micro inches or micrometers. The number of grinding parameter that end user needs to understand is quite limited (Marinescu, 2001).

### 2.6.1 Surface Texture

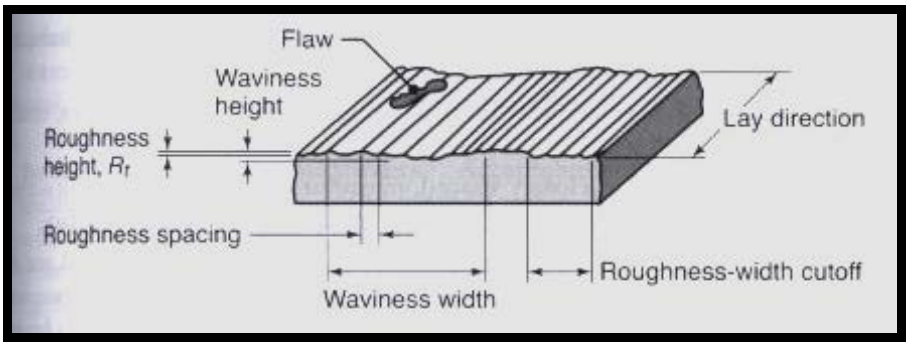


**Figure 2.2 :** Surface texture

Source : (Kalpakjian, 2001)

Due to production, all surfaces have their own characteristics that referred to surface roughness. The description of surface texture as a geometrical property is complex. Due to the study, the understanding of the surface texture is important to the surface analysis. There are several surface textures define by (Kalpakjian, 2001):

a) Flaws or defects are random irregularities such as scratches, cracks, holes, depressions, seams, tears or inclusions (Figure 2.2)
b) Lay or directionality is the direction of the predominant surface pattern and is usually visible to the naked eye.
c) Roughness is defined as closely spaced, irregular deviations on a scale smaller than that of waviness. Roughness is expressed in terms of its heights, its width, and its distance on the surface along which it is measured.
d) Waviness is a recurrent deviation from a flat surface, much like waves on the surface of water.

Research on surface texture in grinding has yielded several factors that affecting ground surface texture (Figure 2.3), (Erik, et al., 2001).

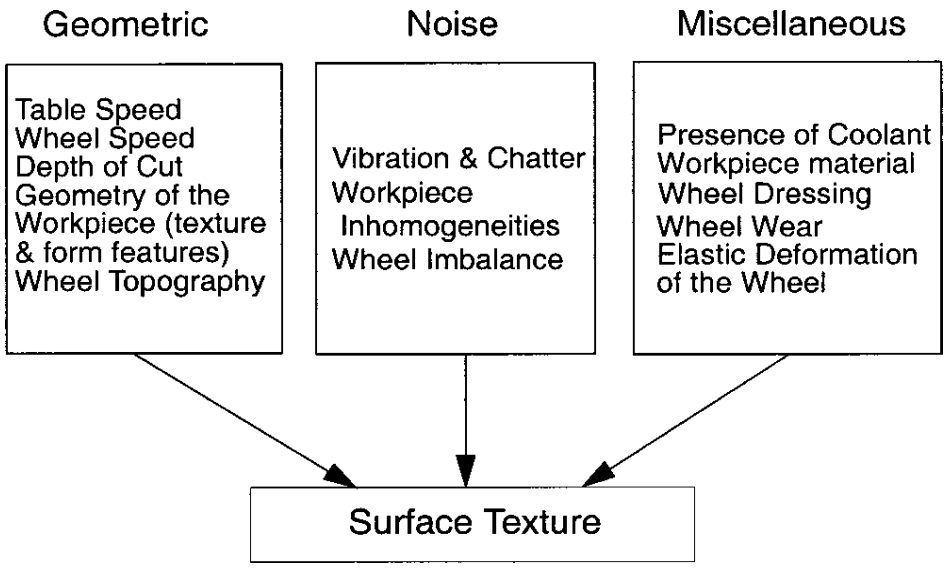


**Figure 2.3:** Classification of Factors Affecting Ground Surface Texture

Source: Erik, et al., 2001

### 2.6.2 Surface Structure and Properties.

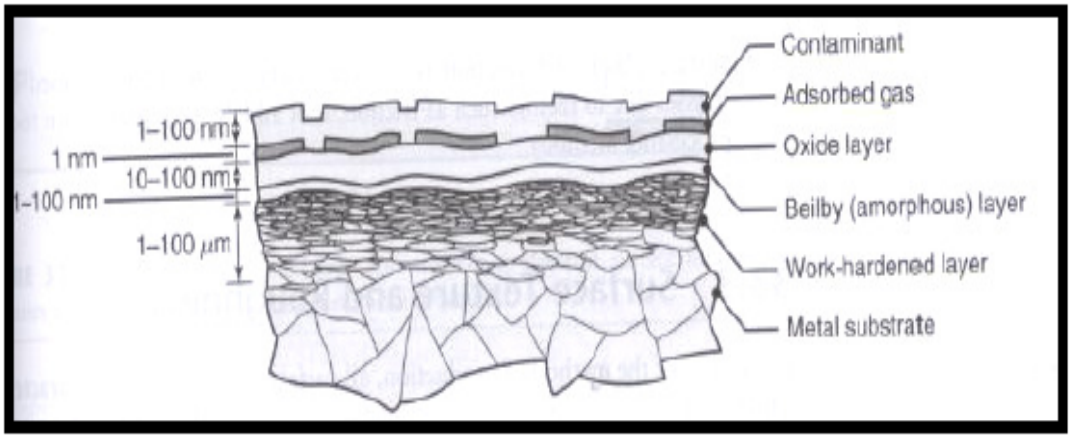


**Figure 2.4:** Illustration of a Cross-Section of the Surface Structure of Metals.

Source: Kalpakjian, 2001.

Based on the metal surface, it is general consists of several layers (Figure 2.4). The characteristic of these layers defined by Kalpakjian (Kalpakjian, 2001):

a) The bulk or metal substrate has a structure that depends on the composition and processing history of the metal.
b) Above bulk metal that usually has been plastically deformed and work-hardened to a greater extent during the manufacturing process. The depth and properties of the work-hardened layer (the surface structure) depend on such factors as the processing method used and how frictional sliding the surface undergoes.
c) Unless the metal is processed and kept in an inert (oxygen-free) environment, or is a noble metal such as gold or platinum, an oxide layer forms over the work hardened layer.
d) Under normal environmental conditions, surface oxide layers are generally covered with adsorbed layers of gas and moisture.
e) Finally, the outermost surface of the metal may be covered with contaminants such as dirt, dust, grease, lubricants residues, cleaning-compound residues, and pollutants from the environments.

### 2.6.3 Surface Roughness Profile Parameters

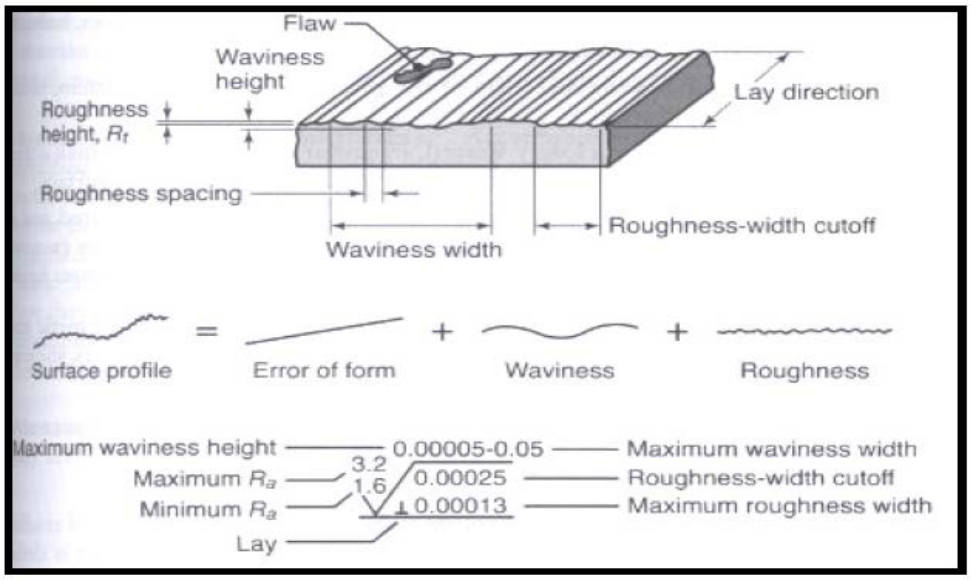


**Figure 2.5:** Standard Terminology and Symbols to Describe Surface Finish

Source: Kalpakjian, 2001

**Roughness Average, Ra**

Ra is the arithmetic average of the absolute values of the roughness profile ordinates (Stefan, 2001). It is also called as Arithmetic Average (AA), Center Line Average (CLA). The average roughness is the area between the roughness profile and its mean line, or the integral of the absolute value of the roughness profile height over the evaluation length.

**Arithmetic Mean, Rz**

Rz is the arithmetic mean value of the single roughness depths of consecutive sampling lengths (Stefan, 2001). Z is the sum of the height of the highest peaks and the lowest valley depth within a sampling length.

**Root-Mean-Square Average, Rq**

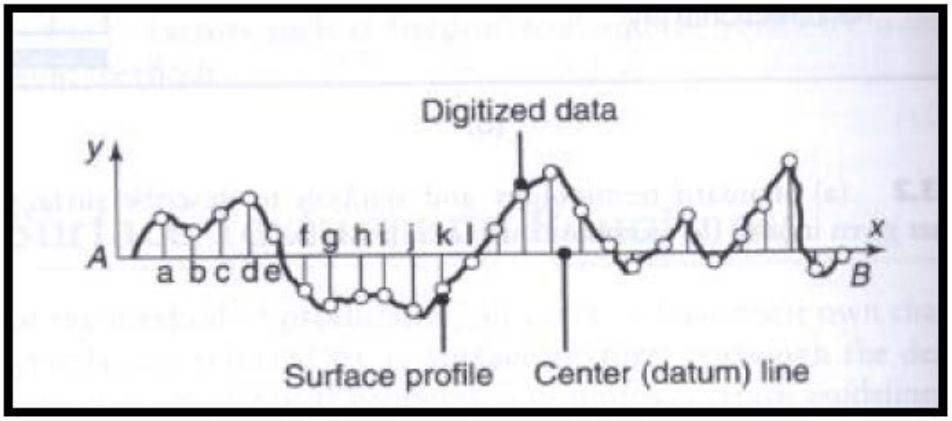


**Figure 2.6:** Coordinates Used Surface Roughness

Source: Stefan, 2001

Rq, formerly identified as RMS is defined as

$$R_q = \sqrt{\frac{a^2 + b^2 + c^2 + d^2 + \cdots}{n}}$$

The datum line AB in Figure 2.6 is located so that the sum of the areas above the line is equal the sum of the areas below the line (Stefan, 2001). The unit used for surface roughness are μm (micrometer or micron) or μin = 0.025μm.

### 2.6.4 Application of Surface Roughness

Surface roughness has been one of the most important quality measures in many mechanical products. The important of surface roughness if often neglected. It has been regarded as being on the fringe general engineering, being looked on as an irritant that has to be dealt with but with not too much trouble (David, 2002). Technologically the importance of materials surface cannot understand since they influence so many factor of modern industry (O'Connor, 2003). Surface found to:

a) Controlling material stability via the corrosion, friction or wear characteristics is automobile components to medical prostheses.

b) Determine material adhesion characteristics.
c) Crucial to systematic process control in materials fabrication such as electronic devices and thin films.
d) Play a vital role in heterogeneous catalytic processes for compound synthesis as in petrochemicals and fertilizers.
e) Control mineral beneficiation via selective floatation and adsorption.
f) Be germane to membrane processes important in numerous diverse fields from environmental control be medicine.

## 2.7 NANOCOOLANT CHARACTERIZATION

Nanocoolant is a new class of fluids engineered by dispersing nanometer-size solid particles into base fluids such as water, ethylene glycol, lubrication oils, and more (Bin Shen, 2008). The recent development of nanocoolants provides alterative cutting fluids which can be used in grinding. The advanced heat transfer and tribological properties of these nanocoolants can provide better cooling and lubricating in the grinding process, and make it production-feasible.

### 2.7.1 Nanocoolant for Cooling Applications

Heat transfers of nanocoolant play an important role for cooling applications. The difference between the cooling and heating cases for the nanofluid is much higher than the associated difference for the pure water ( Kim et al., 2009). Heating of the working fluid provided higher enhancement since thermal conductivity of the working fluid at the wall significantly affects the heat transfer**.** Heat transfer fluids play an important role for cooling applications in many industries including manufacturing, transportation, energy, and electronics. Developments in new technologies such as highly integrated microelectronic devices, higher power output engines, and reduction in applied cutting fluids continuously increase the thermal loads, which require advances in cooling capacity. Therefore, there is an urgent need for new and innovative heat transfer fluids to achieve better cooling performance.

### 2.7.2 Nanocoolants Synthesis

There are mainly two methods of nanocoolant production, namely, two-step technique and one-step technique (Bin Shen, 2008).

One-step technique combines the production of nanoparticles and dispersion of nanoparticles in the base fluid into a single step. There are some variations of this technique. In one of the common methods, named direct evaporation one-step method, the nanofluid is produced by the solidification of the nanoparticles, which are initially gas phase, inside the base fluid (Eastman et al., 2001). The dispersion characteristics of nanocoolants produced with one-step techniques are better than those produced with two-step technique. The main drawback of one-step techniques is that they are not proper for mass production, which limits their commercialization (Choi et al., 2008).

In the two-step technique, the first step is the production of nanoparticles and the second step is the dispersion of the nanoparticles in a base fluid. Two-step technique is advantageous when mass production of nanocoolants is considered, because at present, nanoparticles can be produced in large quantities by utilizing the technique of inert gas condensation (Romano et al., 1997). The main disadvantage of the two-step technique is that the nanoparticles form clusters during the preparation of the nanofluid which prevents the proper dispersion of nanoparticles inside the base fluid (Choi et al., 2008).

### 2.7.3 Heat Transfer in Nanocoolant

Nanocoolants are promising heat transfer fluids due to the high thermal conductivity enhancements (Heris et al., 2006). The possible reason is that the suspensions have higher viscosity than that of pure water, especially at high particle volume fractions. Heat transfer performance of nanocoolant is significantly more dependent on temperature when compared to pure fluids (Kim et al., 2009). However, it has been clearly shown by the available results that the heat transfer behaviour of nanocoolants is very complex and the application of nanocoolants for

heat transfer enhancement should not be decided only by their effective thermal conductivity. Many other factors such as particle size, shape and distribution, micro-convection, pH value, and the particle–fluid interactions should have important influence on the heat transfer performance of the nanocoolants (Xiang et al., 2006).

### 2.7.4 Thermal Conductivity of Zinc Oxide Nanocoolants

Transient hot wire method is widely used to measure thermal conductivity of materials, especially for fluids. It was developed about thirty years ago (Hoshi et al., 1981). Before that time, the thermal conductivity of fluids had historically proven to be a difficult transport property to measure accurately because the heat transfer by convection was recognized as a prominent source of error during the measurement (DeGroot et al., 1974). The most advantageous feature of the transient hot wire method for thermal conductivity measurements of fluids is its capability of experimentally eliminating convective error, and for this reason, it is a high precision technique for the measurement of the thermal conductivity of fluids (Nagasaka and Nagashima, 1981).

Generally, conventional heat transfer fluids have poor heat transfer properties compared to solids. Most solids have orders of magnitude larger thermal conductivities than those of conventional heat transfer fluids (Table 2.3). Therefore, fluids containing suspended solid particles are expected to display significant enhancement in thermal conductivities relative to conventional heat transfer fluids.

Thermal conductivity is the most important parameter responsible for enhanced heat transfer. Based on the review of (Bin Shen, 2008) studies, the thermal conductivity of water-based ZnO nanocoolants increases rapidly with the increase of the particle sizes (Figure 2.6). The results are very similar to those of $Al_2O_3$ nanocoolants. The thermal conductivity enhancement increases with increasing volume fraction of nanoparticles, as well as the increasing particle size. For the ZnO nanocoolant with a particle size of 60 nm, the increase in thermal conductivity is about 61% at the 15 vol%.

**Table 2.4:** Thermal Conductivity of Matters

| Material | Thermal Conductivity (W/m-K) @ 300K |
|---|---|
| ***Metallic solids*** | |
| Copper | 401 |
| Aluminum | 237 |
| ***Non-metallic solids*** | |
| Aluminum Oxide | 36 |
| Zinc Oxide | 100 |
| ***Conventional heat transfer fluids*** | |
| Water | 0.613 |
| Ethylene Glycol | 0.252 |

Source: Incropera and DeWitt, 2001

The thermal conductivity measurement of water-based ZnO nanocoolants with particle sizes of 20, 40, and 60 nm is shown in Figure 2.6. The thermal conductivity enhancement increases with increasing volume fraction of nanoparticles. The improvement of thermal conductivity reaches 15 vol % from 5 vol % of 60 nm ZnO nanoparticles. From experimental data, it is obvious that the 60 nm ZnO nanocoolants have larger thermal conductivity enhancement than 20 nm and 40 nm.

As conclusion of the previous researchers result, the thermal conductivity of nanocoolant is high compared to water fluid. Due to this, the temperature will decrease and enhance grinding performance whereby the surface roughness gets better and the wheel wear reduces.

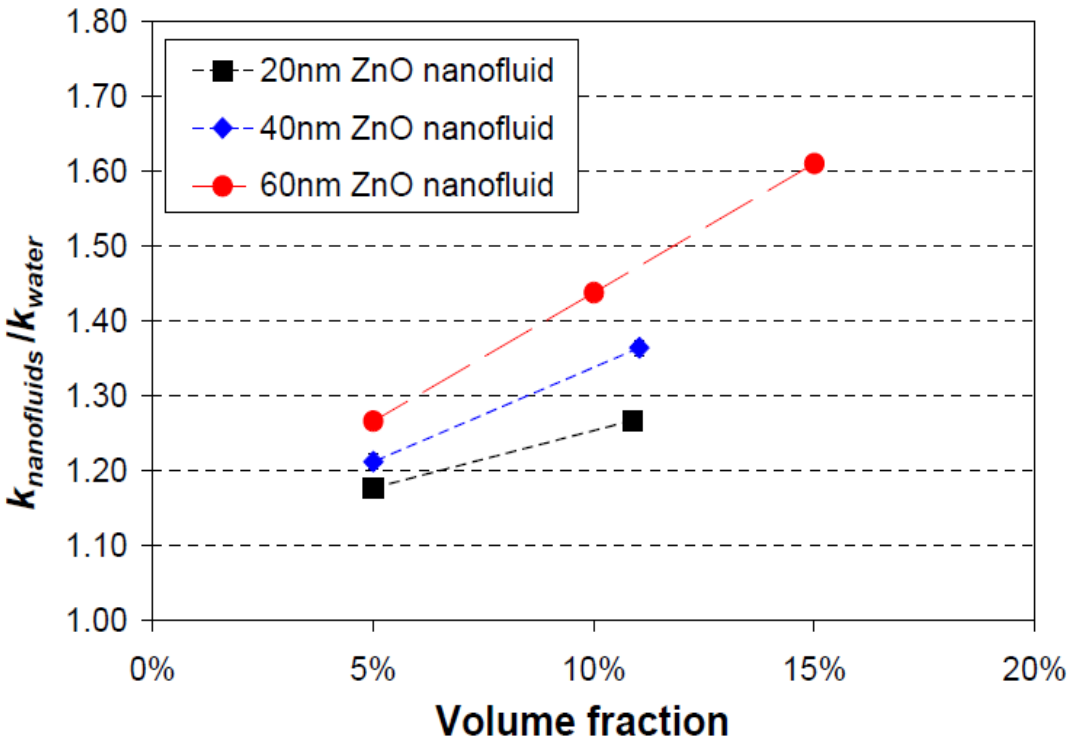


**Figure 2.7:** Thermal Conductivity of High Volume Fraction ZnO Nanocoolants

Source : Bin Shen, 2008

The thermal conductivity of nanocoolants is determined experimentally by many (Eastman et al., 2001, Xie et al., 2002, Kumar Das et al., 2003, Murshed et al., 2005, Hong et al., 2005, Shima et al., 2009). The experiments are conducted mostly with spherical shape particles having diameters in the range of 20 – 150nm, temperature of 20 – 70$^{o}$C and volume concentration less than 4.0%. The thermal conductivity data of Pak and Cho, 1998, Williams et al., 2008, Lee et al., 1999, Murshed et al., 2005, Kumar Das et al., 2003, Chon and Kihm, 2005, Mintsa et al., 2009, Beck et al., 2009, Avsec, 2008, Duangthongsuk and Wongwises, 2009, Sundar et al., 2011 and Hong et al., 2007 for metal and metal oxides such as $Al_2O_3$, $TiO_2$, $Fe_3O_4$, $ZrO_2$, CuO and ZnO nanocoolants consisting of 252 data points available in the literature are used in the development of regression equations. Regression is applied to the data assuming that the complexity associated with the motion of the nanoparticle in the medium is dependent on the $\pi$ - terms given by

$$\frac{k_{nf}}{k_w} = f\left[\pi_1\ ,\ \pi_2\ ,\ \pi_3\ ,\pi_4\right] \tag{2.1}$$

where, $T_{nf}^{*}$ and $d_p^{*}$ are the upper limits of the experimental data related to temperature and nanoparticle diameter chosen as reference values employed in the regression.

$$k_r = \frac{k_{nf}}{k_w} = \left[0.8938\left(1+\frac{\phi}{100}\right)^{1.37}\left(1+\frac{T_{nf}}{70}\right)^{0.2777}\left(1+\frac{d_p}{150}\right)^{-0.0336}\left(\frac{\alpha_p}{\alpha_w}\right)^{0.01737}\right] \tag{2.2}$$

The Equation (2.2) obtained with Average Deviation (AD) of 2.73%, Standard Deviation (SD) of 3.55% and maximum deviation of 10.96%. The properties of water are estimated with the equations listed in Table 3.3. The values of density, specific heat and thermal conductivity of nano materials used in the regression Equation (2.2) are shown as Table 2.5. The correlation equation is validated with the data shown in the legend of Figure 2.8 with a maximum deviation of less than 11% for a few points.

**Table 2.5:** Physical properties of nano materials

| Nanoparticle | Thermal Conductivity, W/m K | Density, kg/m$^3$ | Specific heat, J/ kg K | Reference |
|---|---|---|---|---|
| $Al_2O_3$ | 36 | 3880 | 773 | Pak and Cho, 1998 |
| CuO | 69 | 6350 | 535 | Fotukian and Nasr Esfahany, 2010 |
| SiC | 490 | 3160 | 675 | Kothandaraman and Subramanyam, 2007 |
| $SiO_2$ | 1.4 | 2220 | 745 | Vajjha et al., 2010 |
| $TiO_2$ | 8.4 | 4175 | 692 | Pak and Cho, 1998 |
| ZnO | 29 | 5600 | 514 | Vajjha and Das, 2009, Hong et al., 2007 |
| $ZrO_2$ | 1.7 | 5500 | 502 | Kothandaraman and Subramanyam, 2007 |

**Table 2.6:** Properties of water applicable in the range $5 \le T_w \le 100\ ^{o}\text{C}$

| **Property** | **Equation for water** |
|---|---|
| Density | $\rho_w = 1000 \times \left[1.0 - \frac{(T_b - 4.0)^2}{119000 + 1365 \times T_b - 4 \times (T_b)^2}\right]$ $\pm 0.07\%$ (Kravchenko, 1966) |
| Viscosity | $\mu_w = 0.00169 - 4.25263e-5 \times T_w + 4.9255e-7 \times (T_w)^2 - 2.0993504e-9 \times (T_w)^3$ $\pm 2.75\%$ |
| Thermal conducti-vity | $k_w = 0.56112 + 0.00193 \times T_w - 2.60152749e-6 \times (T_w)^2 - 6.08803e-8 \times (T_w)^3$ $\pm 1.4\%$ |
| Specific heat | $C_w = 4217.629 - 3.20888 \times T_b + 0.09503 \times (T_b)^2 - 0.00132 \times (T_b)^3 + 9.415e-6 \times (T_b)^4 - 2.5479e-8$ $\pm 2.46\%$ |

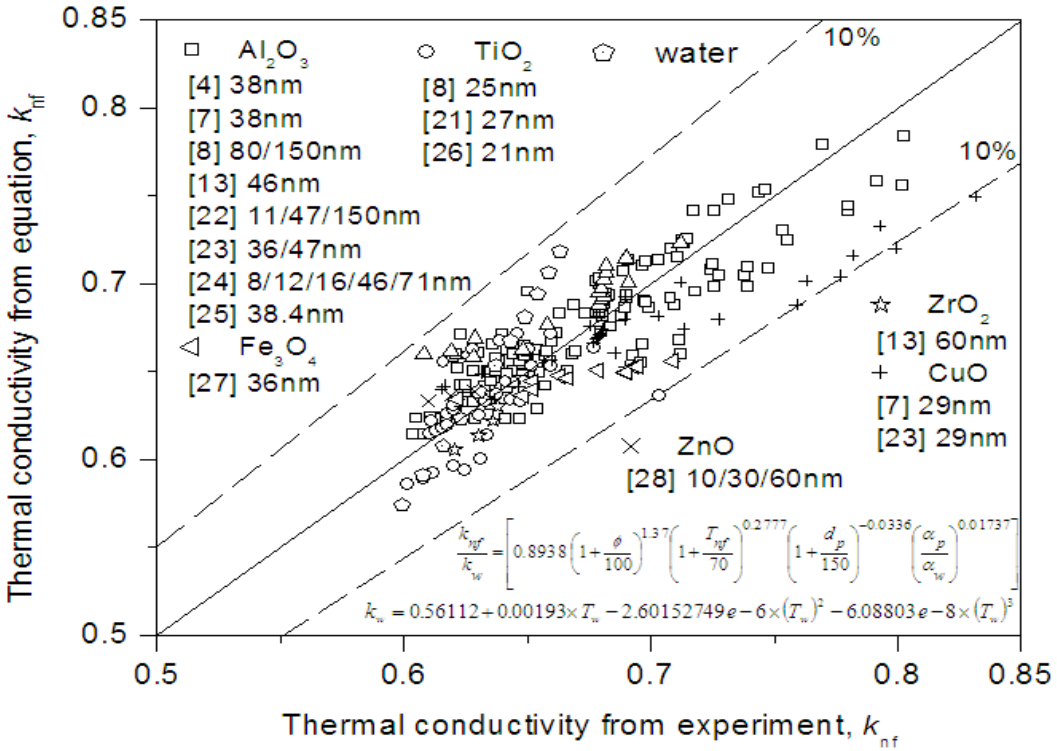


**Figure 2.8:** Validation of data with the Equation (2.1)

(Source: Sharma, 2012)

### 2.7.5 Viscosity in Nanocoolant

The viscosity water nanocoolants as a function of shear rate were measured by (Ding et al., 2005). They observed that the viscosity of nanocoolants decreased with increasing temperature. That means the nanocoolants can provide better fluid flow performance due to the higher shear rate at the wall, which results in low viscosity there. It can perform as a better lubricating fluid. For the same flow rate, the Reynolds number would be lower if the fluid has a higher viscosity. Therefore, the nanocoolants with higher viscosity have the higher Nusselt number under the same Reynolds number, which is actually corresponding to a higher flow rate (Bin Shen, 2008). The high volume fraction of nanocoolant results in the high viscosity. Based on the research by (Bin Shen, 2008), the 4.0 vol% nanocoolant is already on the high side of concentration compared with 1.0 vol % and 3.0 vol %, because of the noted increase in viscosity.

Nguyen et al., 2007 conducted experiments for the determination of viscosity of $Al_2O_3$ and CuO nanocoolants in water at different concentrations and particle sizes under ambient conditions. The authors have stated that the viscosity of $Al_2O_3$ nanocoolant with particle size of 36 and 47nm and CuO of 29nm size predicted close values for volume concentration less than 4% and deviated at higher concentrations. Hence the experimental data of viscosity obtained by Nguyen et al., 2007, Hwang et al., 2009, Wang et al., 1999, Zeinali Heris et al., 2006, Nguyen et al., 2008, Lee et al., 2008, Pak and Cho, 1998, He et al., 2007, Duangthongsuk and Wongwises, 2010 and Lee et al., 2011 having volume concentration less than 4%, consisting of 233 data points are subjected to regression and the following correlation obtained.

$$\mu_r = \frac{\mu_{nf}}{\mu_w} = C_1 \left(1 + \frac{\phi}{100}\right)^{11.3} \left(1 + \frac{T_{nf}}{70}\right)^{-0.038} \left(1 + \frac{d_p}{170}\right)^{-0.061} \tag{2.3}$$

Equation (2.3) is validated with the experimental data, shown as Figure 2.9 with $C_1 = 1.4$ for SiC and $C_1 = 1.0$ for other water based nanocoolants. The data could be correlated with an average deviation of 3.18%, standard deviation of 3.8% and a maximum deviation of 13%. Thus, having established Eqs (2.3) and (2.3) for the

estimation of nanocoolant properties, the application of these relations in evaluating friction and heat transfer coefficients for turbulent flow will be undertaken.

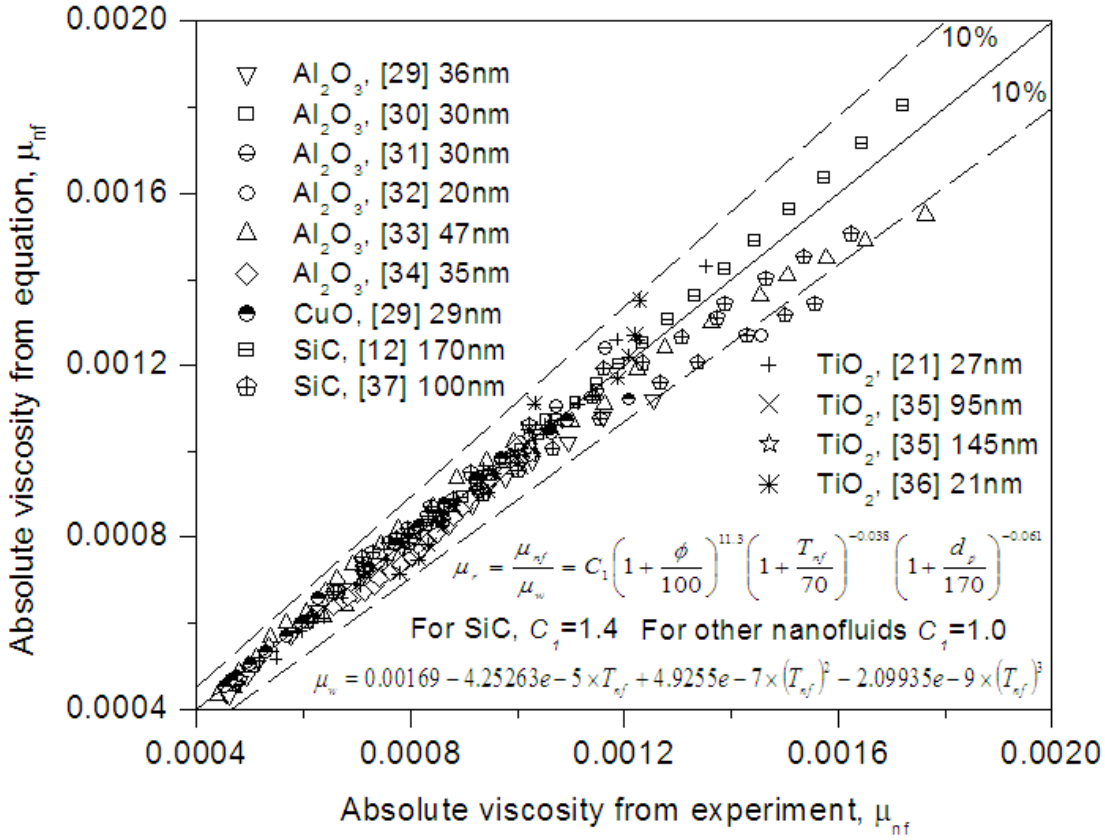


**Figure 2.9:** Validation of data with the equation (2.2)
(Source: Sharma, 2012)

The primary consideration of the report is to review the salient physical properties of nanocoolants and establish generalized correlations for water based nanocoolants for particle sizes varying between 2—120 nm. It is fairly established from the regression analysis that the thermal conductivities and absolute viscosities of nanocoolants are dependent on volumetric concentrations and temperature of the medium. The influence of particle size hither to not account for might also be an influencing factor. These relationships are subsequently used in the evaluation of friction and heat transfer coefficients, to validate the correctness of the correlations.

## 2.8 NEURAL NETWORK

The research returned by (Demuth, et al., 2002) stated that the neural networks are composed of simple elements operating in parallel. These elements are inspired by biological nervous systems. As in nature, the network function is determined largely by the connections between elements. Commonly neural networks are adjusted, or trained, so that a particular input leads to a specific target output. Neural networks have been trained to perform complex functions in various fields of application including pattern recognition, identification, classification, speech, vision and control systems.

In its most general form, a neural network is a machine that is designed to model the way in which the brain performs a particular task or function of interest; the network is usually implemented using electronic components or simulated in software on a digital computer. Our interest will be confined largely to neural networks that perform useful computations through a process of learning. To achieve good performance, neural networks employ a massive interconnection of simple computing cells referred to as neurons or processing units (M.Hajek, 2005).

## 2.9 Benefits of Neural Network

It is apparent from the above discussion that a neural network derives its computing power through, first, its massively parallel distributed structure and, second, its ability to learn and, therefore, generalize. Generalization refers to the neural network producing reasonable outputs for inputs not encountered during training. These two information processing capabilities make it possible for neural networks to solve complex (large-scale) problems that are currently intractable. In practice, however, neural networks cannot provide the solution working by themselves alone. Rather, they need to be integrated into a consistent system engineering approach. Specifically, a complex problem of interest is decomposed into a number of relatively simple tasks, and neural networks are assigned a subset of the tasks (e.g. pattern recognition, associative memory, control) that match their inherent capabilities. It is important to recognize, however, that we have a long way

to go before we can build a computer architecture that mimics a human brain. The use of neural networks offers the following useful properties and capabilities:

### 2.9.1 Nonlinearity

A neuron is basically a nonlinear device. Consequently, a neural network, made up of an interconnection of neurons, is itself nonlinear. Moreover, the nonlinearity is of a special kind in the sense that it is distributed throughout the network.

### 2.9.2 Adaptivity

Neural networks have a built-in capability to adapt their synaptic weights to changes in the surrounding environment. In particular, a neural network trained to operate in a specific environment can be easily retrained to deal with minor changes in the operating environmental conditions. Moreover, when it is operating in a non stationary environment a neural network can be designed to change its synaptic weights in real time. The natural architecture of a neural network for pattern classification, signal processing, and control applications, coupled with the adaptive capability of the network, makes it an ideal tool for use in adaptive pattern classification, adaptive signal processing, and adaptive control.

### 2.9.3 Input-output mapping

A popular paradigm of learning called *supervised learning* involves the modification of the synaptic weights of a neural network by applying a set of training samples. Each sample consists of a unique input signal and the corresponding desired response. The network is presented a sample picked at random from the set, and the synaptic weights (free parameters) of the network are modified so as to minimize the difference between the desired response and the actual response of the network produced by the input signal in accordance with an appropriate criterion. The training of the network is repeated for many samples in the set until the network reaches a steady state, where there are no further significant changes in the synaptic weights.

The previously applied training samples may be reapplied during the training session, usually in a different order. Thus the network learns from the samples by constructing an input-output mapping for the problem at hand.

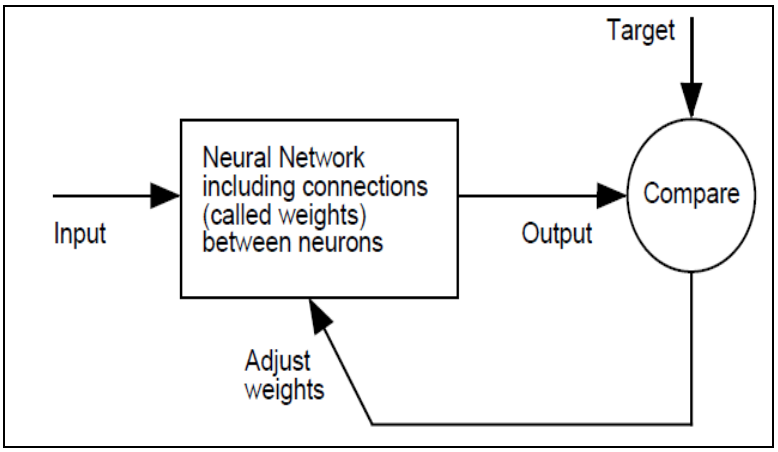


**Figure 2.10:** Neural Network Connection

### 2.9.4 Contextual information

Knowledge is represented by the very structure and activation state of a neural network. Every neuron in the network is potentially affected by the global activity of all other neurons in the network. Consequently, contextual information is dealt with naturally by a neural network.

### 2.9.5 Fault tolerance

A neural network, implemented in hardware form, has the potential to be inherently fault tolerant in the sense that its performance is degraded gracefully under adverse operating. For example, if a neuron or its connecting links are damaged, recall of a stored pattern is impaired in quality. However, owing to the distributed nature of information in the network, the damage has to be extensive before the overall response of the network is degraded seriously. Thus, in principle, a neural network exhibits a graceful degradation in performance rather than catastrophic failure.

# CHAPTER 3

# METHODOLOGY

## 3.1 INTRODUCTION

This chapter is the overview of the experimental work of grinding using conventional abrasive wheel of silicon carbide to grind aluminium alloy with zinc oxide nanocoolant. This experimental procedure utilized to predict the grinding machinability. Water based nanocoolant were employed in grinding and the performance will be evaluated in terms of surface roughness and wheel wear.

Flowchart system detailing the task need to complete was drafted out. This flow chart (Figure 3.1) shows the overall flow of project in step by step process. There must have a triangular in the flowchart, means that the result obtain from the experiment can be change if the result if failure. Due to that, the experimental procedure needs to conduct again until the expected result is achieved.

The design of the experiment is a main task need to consider in this chapter. In this study, the design of the experiment is using one conventional wheel (silicon carbide). The numbers of experiment for the wheel are nine for single-pass and another nine for multi-pass. Then, prepare the apparatus and equipment that needed for the experiment.

## 3.2 FLOW CHART

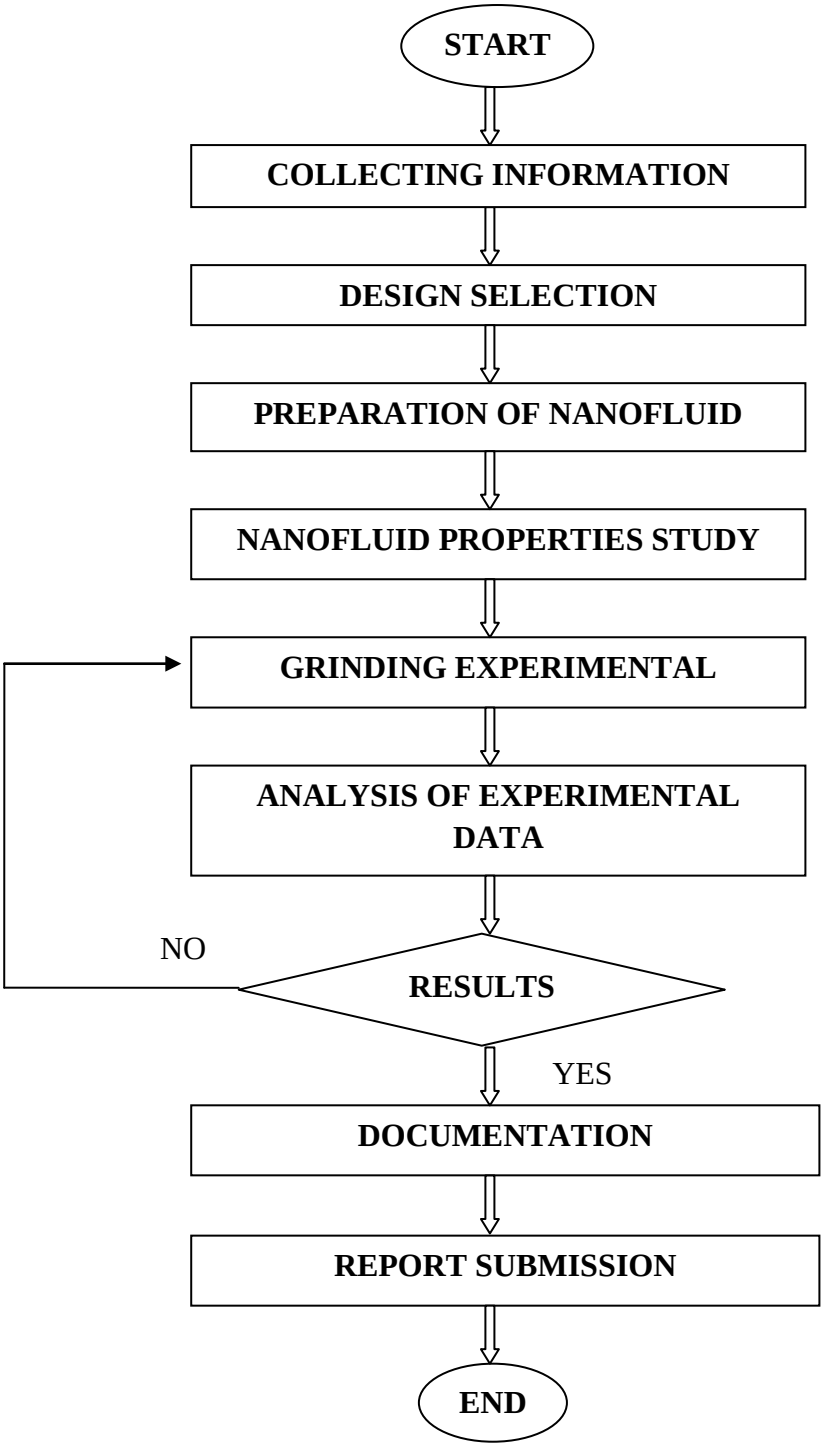


**Figure 3.1:** Process Flow Chart of Study

## 3.3 FLOW CHART DESCRIPTIONS

The flowchart above describes the overall flow of process in step by step. Each step in the flowchart will be discussed briefly in the upcoming sub-topic.

### 3.3.1 Collecting Information

The equipment used for the grinding process was surface grinding machine model SUPERTEC STP1022ADCII (Figure3.2). The grinding wheel used was silicon carbide (Figure 3.3). The perthometer (Figure 3.4) was used to measure the surface roughness. The tachometer (Figure 3.5) was used to maintain the work speed at 200rpm. The optical microstructure (Figure 3.6) was used to measure the 2D microstructure of the material. Based on the parameter used, the design of experiment was decided. There are two type of experiment conducted which are single-pass and multi-pass, and there are eighteen experiment conducted for each pass.

**Table 3.1:** Specification of Surface Grinding Machine

| | |
|---|---|
| **Controlling Mode** | CNC |
| **Processing Types** | Metal |
| **Automatic Grade** | Automatic |
| **Table size** | 200x500mm |
| **Max grinding length** | 550mm |
| **Max grinding width** | 210mm |
| **Manual traverse** | 620mm |
| **Hydraulic traverse** | 570mm |
| **Manual travel** | 250mm |
| **Rapid traverse** | (60hz / 50hz) 960/800mm/min |
| **Grinding wheel Dia x Width x Bore** | Ø205x22xØ32mm |
| **Spindle speed** | (60hz / 50hz)3420/2850rpm |
| **Spindle motor** | 2 hp |
| **Machine weight** | 1300kgs |

**(SUPERTEC STP1022ADCII)**


**Figure 3.2 :** Surface Grinding Machine (SUPERTEC STP1022ADCII)

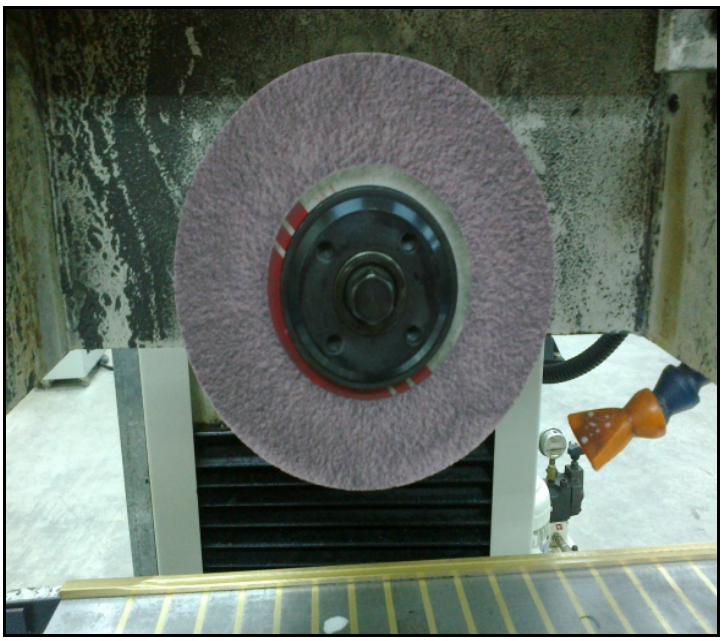

**Figure 3.3:** Grinding Wheel - Silicon Carbide


**Figure 3.4 :** Perthometer

**Figure 3.5:** Tachometer


**Figure 3.6:** Optical Measurement

### 3.3.2 Design Selection

The design that has been selected for this project was a rectangular shape of workpiece aluminium alloy 6061 with the usage of zinc oxide nanocoolant as cutting fluid (Figure 3.8). The rectangular shape of work piece was selected for the ease of grinding process. The material was used for the surface roughness testing microstructure observation. The zinc oxide nanocoolant was used as coolant to replacing water based coolant for grinding.

### 3.3.3 Preparation of Nanocoolant

First, distilled was prepared for nanocoolant dilution process. Aquamatic Water Still was used as an equipment to prepare distills water in this project (Figure 3.7). First, on the water supply pipe and ensure the volume of water contain in the heater is on the top level. Next, on the power supply and leave the water in the heater to be vaporized by the metal heater. The steam of the vaporized water will be cooled

in the boron silica glass. The cooled steam will be produced as distilled water. The distilled water will be transferred to the tank to use for the nanocoolant preparation.

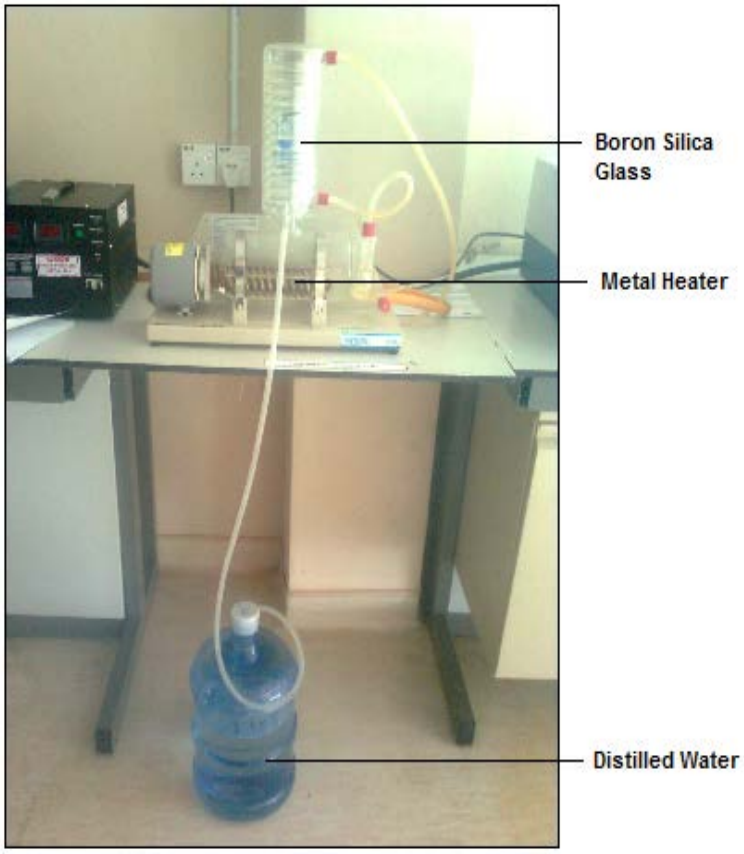


**Figure 3.7:** Aquamatic Water Still

The preparation of nanofluid is very important because this fluid will be used as cutting fluid for the grinding process. There are mainly two methods of nanofluid production, namely, two-step technique and one-step technique. The method used for nanofluid preparation in this project was a one step preparation. The nanofluid can be diluted in two ways which are by weight or by volume. In this project, the preferred way for the dilution is by volume. In these studies, zinc oxide nanofluid is used as cutting fluid.

The properties such as viscosity and thermal conductivity of the nanocoolant are estimated. The concentration of the nanocoolant expressed in terms of volume percent, $\phi$ is estimated with Eq. (3.1). The nanocoolant is procured from Sigma-

Aldrich which is available in weight concentration and listed in Table 3.2. The nanocoolant concentration in weight percent, $\omega$ is converted into volume percent using Eq. (3.2). The equivalent value of volume percent concentration is shown in Table 3.2 (Sources: Sigma-Aldrich).

$$\phi = \left(\frac{m_p}{\rho_p}\right) \Big/ \left(\frac{m_p}{\rho_p} + \frac{m_w}{\rho_w}\right) \times 100 \tag{3.1}$$

$$\phi = \frac{\omega \rho_w}{\left(1 - \frac{\omega}{100}\right)\rho_p + \frac{\omega}{100}\rho_w} \tag{3.2}$$

Where, $$\omega = \left[m_p / \left(m_p + m_w\right)\right] \times 100 \tag{3.3}$$

$$\phi 1 = \frac{\phi \rho_w}{\left(1-\phi\right)\rho_p + \phi \rho_w} \tag{3.4}$$

The properties of the nanoparticle are listed in Table 2.6. The required volume concentration can be estimated by adding water to the existing nanocoolant available in volume percent concentration using the relations given by Eq. (3.5).

$$\Delta V = V_1 \left(\frac{\phi_1}{\phi_2} - 1\right) \tag{3.5}$$

Where, $\Delta V = V_2 - V_1$; volume of DW into the nanocoolant

$V_1$; initial volume

$V_2$; final volume

$\phi_1$; volume percent before dilution

$\phi_2$ ; volume percent after dilution

**Table 3.2:** Properties of nanocoolants supplied by Sigma Aldrich

| Type of Nanocoolants | Diameter (nm) | Weight Concentration $\omega$ (%) | Volume Concentration $\phi$ (%) |
|---|---|---|---|
| $Al_2O_3$ | 50 | 20 | 6.05 |
| ZnO | 100 | 50 | 15.15 |
| TiO2 | 150 | 35 | 11.42 |

**Calculation of zinc oxide nanofluid concentration**

| $\rho_{water}$ | $\rho_{particle}$ | $V_{1,zinc\ oxide}$ (ml) | $\phi_{ZnO\ nanoparticle}$ |
|---|---|---|---|
| 1000 kg/m$^3$ | 5600 kg/m$^3$ | 60+60+60=180 | 50 wt % (0.5 wt) |
| $\phi_1$ = Initial concentration of ZnO nanofluid (by volume)<br>$\phi_2$ = Final concentration of ZnO nanofluid (by volume %) | | | |

1. Expression for conversion of wt, ϕ to vol, ϕ, (Eq 3.3).

$$\phi_1 = \frac{\phi \rho_w}{(1-\phi)\rho_p + \phi \rho_w}$$

$$= \frac{(0.5)(1000)}{(1-0.5)(5600)+(0.5)(1000)}$$

= 0.1515 vol

2. Expression for total amount distilled water to be added, (Eq 3.5).

$$\Delta V = V_1\left(\frac{\phi_1}{\phi_2} - 1\right)$$

$$\Delta V = 180\left(\frac{0.1515}{0.001} - 1\right)$$

$$\Delta V = 27090 \text{ ml}$$

The steps for the nanocoolant preparation are as below:

a) First, prepare the equipment (motorized stirrer, three bottles of zinc oxide nanoparticle, tank, 500ml beaker) for the nanocoolant dilution.
b) Measure the total volume of the nanofluid contain in the three bottles. It was 180ml.
c) The estimated concentration for the nanocoolant after dilution should be 0.1 vol %. This concentration is just good enough to run the experiment.
d) Then, calculate the volume of distilled water needed for the dilution of 0.1 vol % concentration nanocoolant. The calculated volume of distilled water was 27090ml. (Calculation as above).
e) Next, a tank was filled with 27090ml of distilled water was prepared under a motorized stirrer.
f) The 180ml zinc oxide nanocoolant was poured into the tank slowly while the stirrer is stirring the mixture (Figure 3.8).
g) The mixture was stirred for one hour for homogenization with the speed of 1000rpm.
h) Then, the zinc oxide nanocoolant of 0.1 vol % concentration and 27270ml was prepared (Figure 3.98).
i) Label the tank and leave the nanofluid in the tank for two week to get a stable nanocoolant for properties study.

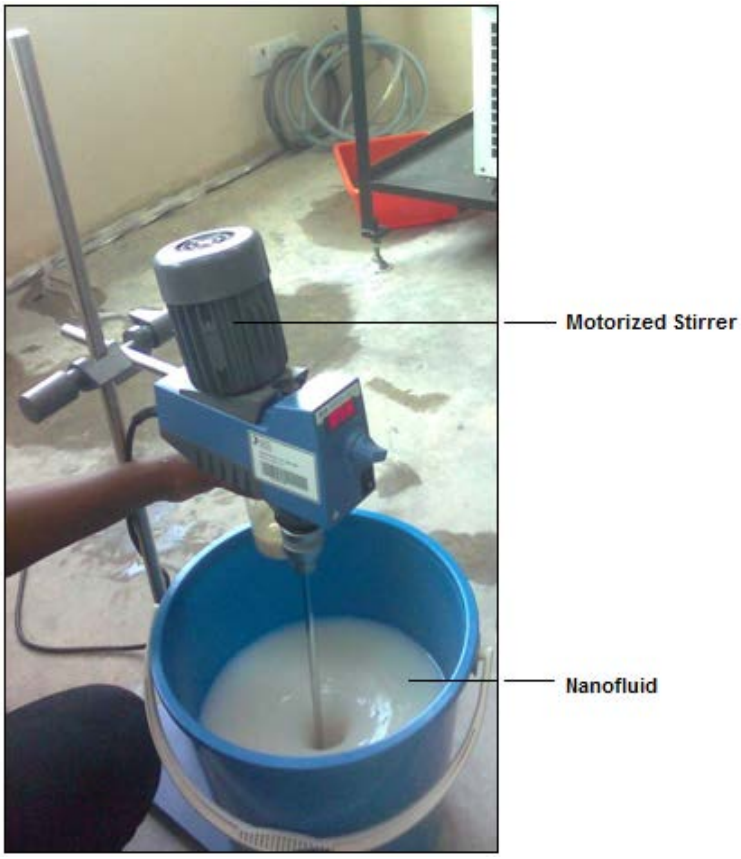


**Figure 3.8:** Stirring Nanocoolant

**Figure 3.9:** Zinc Oxide Nanocoolant

### 3.3.4 Nanocoolant Properties Study

In this study, the properties on nanofluid need to be investigated. The properties of nanocoolant affect the grinding process. Nanofluid will be defined in properties term of thermal conductivity and viscosity.

The thermal conductivity of nanofluid was measured using KD2 Pro thermal property analyzer (Decagon Devices, Inc., USA). It consists of a handheld controller (microcontroller and power control) and three separate sensors (heating element and thermistor) for solid and liquid. The thermal conductivity measurement assumes the long heat source can be treated as an infinite line heat source. The sample medium is isotropic and homogeneous solution. The initial temperature of the sample is assumes constant. Even though the assumptions are not reflecting to the real measurement condition, they are sufficient for accurate thermal conductivity measurements.

The KS-1 sensor needle was used in the thermal conductivity measurement. It was made by stainless steel with 60 mm long and 1.3 mm diameter. The sensor needle dimension is closely approximates the infinite line heat source which gives least disturbance to the sample during measurements. It is designed primarily for liquid samples in the range of 0.2 to 2.00 W/m.K with an accuracy of ±5%. The KD2 Pro uses the transient line heat source method to measure thermal properties of fluid sample. The KD2 Pro takes measurements at 1-second intervals during a 90-second measurement cycle. A 30 second heat pulse is applied to a needle, and the temperature response with time is monitored either at the heated needle or at an adjacent needle. During the first 30 s, the instrument will equilibrate which is then followed by heating and cooling of sensor needle for 30 s each. It then analyzes the data and corrects for sample temperature drift to providing accurate thermal properties measurements. At the end of the reading, the controller computes the thermal conductivity using Eq. (3.6).

$$k = \frac{q\left[\ln(t_2) - \ln(t_1)\right]}{4\pi(\Delta T_2 - \Delta T_2)} \tag{3.6}$$

where $q$ is constant heat rate applied to an infinitely long and small "line" source, $\Delta T_1$ and $\Delta T_2$ are the changes in the temperature at times $t_1$ and $t_2$, respectively.

The calibration of the sensor needle was carried out first by measuring thermal conductivity of distilled water and glycerin. The measured values at room temperature for distilled water, glycerin and ethylene glycol were 0.610 and 0.280 W/mK, respectively, which are in agreement with the literature values of 0.613 and 0.285 W/mK, respectively, within ± 5% accuracy. In non-viscous (Newtonian) fluids (mostly nanofluid at low concentration), heat transfer by convection can be much greater than heat transfer by conduction. The steps can be taken to minimize both forced and free convection heat transfer in the measured sample; i) Ensure that there is no shaking, mixing, or vibration of the fluid during or immediately before the measurement. ii) Vertical insertion of the probe into the fluid will minimize errors from free convection. iii) Less viscous fluids are more subject to errors from free convection. Low viscosity fluids must be stabilized before measurement with the KD2 sensor. Figure 3.10 shows the KD2 Pro components. 1 – Sample bottle, 2 – sensor, 3 – cap, 4 – cable, 5 – microcontroller.

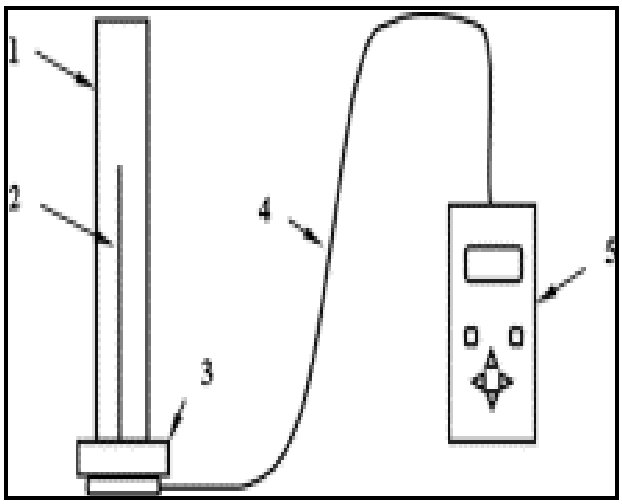


**Figure 3.10 :** Kd2 Pro Components

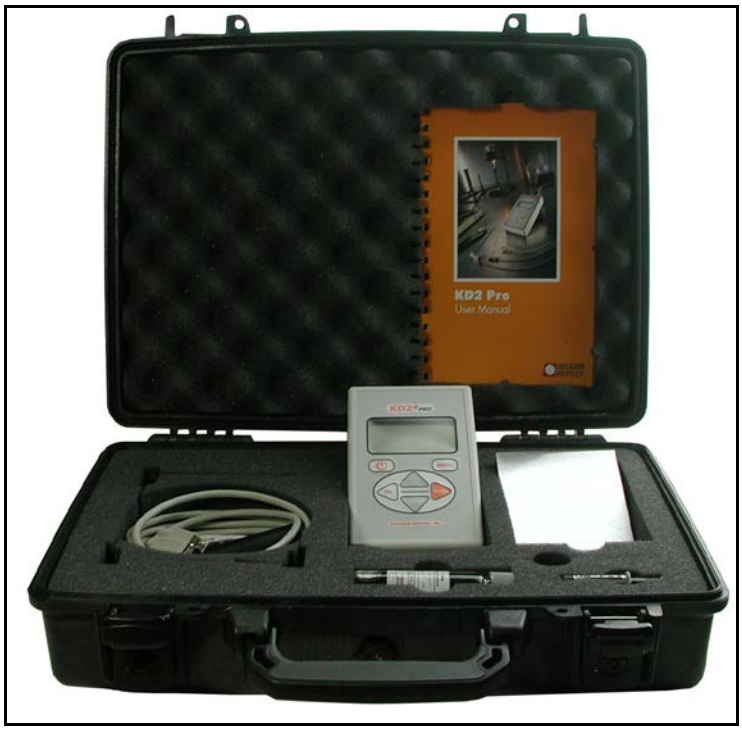


**Figure 3.11:** KD2 Pro Transient Hotwire Thermal Conductivity Meter

The viscosity of the nanofluid was measured using Brookfield LVDV-III Ultra Rheometer (Figure 3.12). $Al_2O_3$/water, ZnO/water and TiO2/water nanocoolants having particle diameters of 50nm, 100nm and 150nm, respectively and up to 6% volume concentrations were used for thermal conductivity and viscosity measurements. The measurements are taken at the room temperature. The principle of operation of the DV-III Ultra is to drive a spindle (which is immersed in the test fluid) through a calibrated spring. Spindle used was SC4-18 which can be used for samples in the viscosity range of 1.0–100 cP. The viscous drag of the fluid against the spindle is measured by the spring deflection. Spring deflection is measured with a rotary transducer.

The viscosity measurement range of the DV-III Ultra (in centipoise or cP) is determined by the rotational speed of the spindle, the size and shape of the spindle, the container the spindle is rotating in, and the full scale torque of the calibrated spring. The small sample adapter requires a sample volume of only 6 - 8 ml (varies with type of spindle) and hence the temperature equilibrium is achieved rapidly

within a minute. The speed range of the viscometer is 1 – 250 rpm. The spindle type and speed combination will produce satisfactory results when the applied torque is between 10% and 100% of the maximum permissible torque. Hence during measurements, the readings were discarded if the applied torque does not fall within this prescribed range. The viscometer was benchmarked with distilled water at room temperature. The measured values of viscosity for distilled water were 0.85, which agree well with the literature values of 0.9, with ±6% accuracy.

In taking viscosity measurements with the DV-III Ultra Rheometer there are two considerations which pertain to the low viscosity limit of effective measurement. i) Viscosity measurements should be accepted within the equivalent % Torque Range from 10% to 100% for any spindle/speed combination. ii) Viscosity measurements should be taken under laminar flow conditions, not under turbulent flow conditions.


**Figure 3.12:** Ultra Rheometer

The first consideration has to do with the precision of the instrument. All DV-III Ultra Rheometers have a full scale range precision of (+/-) 1% of any spindle/speed combination. We discourage taking readings below 10% of range

because the potential viscosity error of (+/-) 1% is a relatively high number compared to the instrument reading. The second consideration involves the mechanics of fluid flow. All rheological measurements of fluid flow properties should be made under laminar flow conditions. Laminar flow is flow wherein all particle movement is in layers directed by the shearing force. For rotational systems, this means all fluid movement must be circumferential. When the inertial forces on the fluid become too great, the fluid can break into turbulent flow wherein the movement of fluid particles becomes random, and the flow cannot be analyzed with standard math models. This turbulence creates a falsely high Rheometer reading, with the degree of non-linear increase in reading being directly related to the degree of turbulence in the fluid.

### 3.3.4 Grinding Process

The grinding process in this project will be handled with the usage of aluminium alloy as the grinding work piece and water based zinc oxide nanocoolant as the coolant. The tank of coolant in the grinding machine contains water based coolant. Therefore, the tank content needs to change to nanofluid. There are two ways that can be applied to change the water based coolant to nanofluid:

a) Change the coolant tank to new tank

b) Use the current tank, suck out the water based coolant and fill with nanofluid.

The first method will be use in this study, whereby change the coolant tank to the new tank. This can reduce the effort for cleaning the current tank that contains water based coolant. First, 27270ml of zinc oxide nanofluid was filled in a new tank. Then, a pipe was fixed with a pump and the pump was placed inside the tank (Figure 3.13). The other end of the pipe was directed to the material to produce coolant when grinding process occurs. A funnel was fixed on the cover of the tank, and the funnel was covered with a towel to filter out the dust and chip produced during grinding process. The nanofluid need to be filter out to maintain the stability and properties of

the nanofluid. The coolant must remain clean and stable because the coolant is recyclable for each experiment.

To start the grinding process, the equipment was prepared which were the surface grinding machine and aluminium alloy, grinding wheel (silicon carbide), vernier caliper, and dressing wheel. First, the wheel dresser (Figure 3.14) was used for the wheel dressing. Then, the wheel diameter was measured using vernier caliper, so that can compare the diameter before and after the experiment to predict the wheel wear. Clamp the aluminium alloy work piece at the correct position down the grinding wheel. Make sure the magnetic chuck was engaged. Next, hand wheel was used for set up the depth of cut. The grinding wheel was turned on and the coolant flow was switched on, and the grinding process was handled. After the required depth of cut was completely grind, the wheel diameter was measured again. Finally, perthometer was used to measure the surface roughness of the work piece at the grinded area and the 2D microstructure was observed for depth of cut (5, 11, and 21) µm for both single and multi-pass. Repeat the procedure for different depth of cut by varying experiment type which were single-pass and multi-pass (Table 3.3). Surface grind the material before start each experiment. Use result from all of the experiment to predict the surface roughness and wheel wear.

| **Grinding Wheel** | Silicon Carbide | | |
|---|---|---|---|
| **Experiment Type** | Single-pass | Multi-pass | |
| **Depth of Cut (µm)** | 5 | 7 | 9 |
| | 11 | 13 | 15 |
| | 17 | 19 | 21 |

**Table 3.3:** Experiment Design

**Figure 3.13 :** Fixing the Coolant Pipe

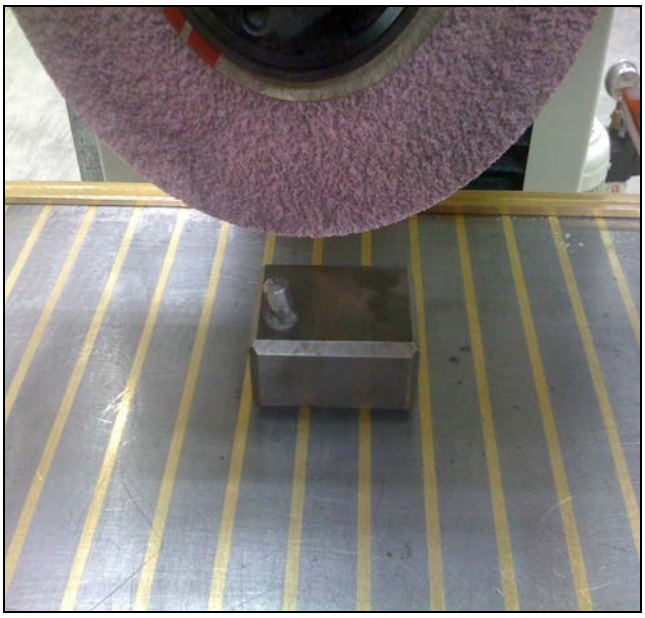

**Figure 3.14:** Wheel Dresser

### 3.3.6 Analysis of Experimental Data

The experimental data was analyzed using Neural Network. Neural networks have been trained to perform complex functions in various fields of application including pattern recognition, identification, classification, speech, vision and control systems (Demuth, et al., 2002). Neural network used to analyse the obtained target and predict the output. Besides, the future prediction also can be carried out with neural.

First, the result of the grinding process needs to save in Microsoft Excel in CSV (Comma Delimited) format. Then, the excel file was opened in the Alyuda NeuroIntelligence, which was the software of neural analysis. The training algorithm used in this study was Limited Memory Quasi-Newton. Before start the analysis, design of fitness criteria was set to r-squared. Then analyse the result and start train the result with various iteration value. Next, test the result and the correlation, r-squared value and a graph obtained. The r-squared value must be above 0.85 in order to get a more accurate graph. The graph of output and target trend must be similar to achieve a good prediction result. The analysis was repeated by changing the iteration value to get a better prediction result. Finally, the surface roughness for various depth of cut was predicted using query and the result was tabulated.

# CHAPTER 4

# RESULTS AND DISCUSSION

## 4.1 INTRODUCTION

This chapter mainly discuss about the results obtained during the experiment and also the possible causes. The nanocoolant properties also will be discussed. The tests that have been done for these grinding processes are surface roughness test and also the wheel wear.

## 4.2 NANOCOOLANT PROPERTIES

The nanocoolant properties result will be discussed briefly in this chapter. The present thermal conductivity equation is compared with other equations from literature.

### 4.2.1 Thermal Conductivity

Comparison of the experimental data of measured thermal conductivity of $Al_2O_3$/water and ZnO/water nanocoolants with values was evaluated as shown in Figure 4.1. The figure shows the measured data of 50nm $Al_2O_3$/water nanocoolant with a maximum deviation of 1.0%. Also the experimental data of ZnO/water nanocoolants with 100nm particle diameter gives an average deviation of 0.9%. A

satisfactory agreement between the two can be observed from the figure indicating the validity of the equations proposed for thermal conductivity estimation.

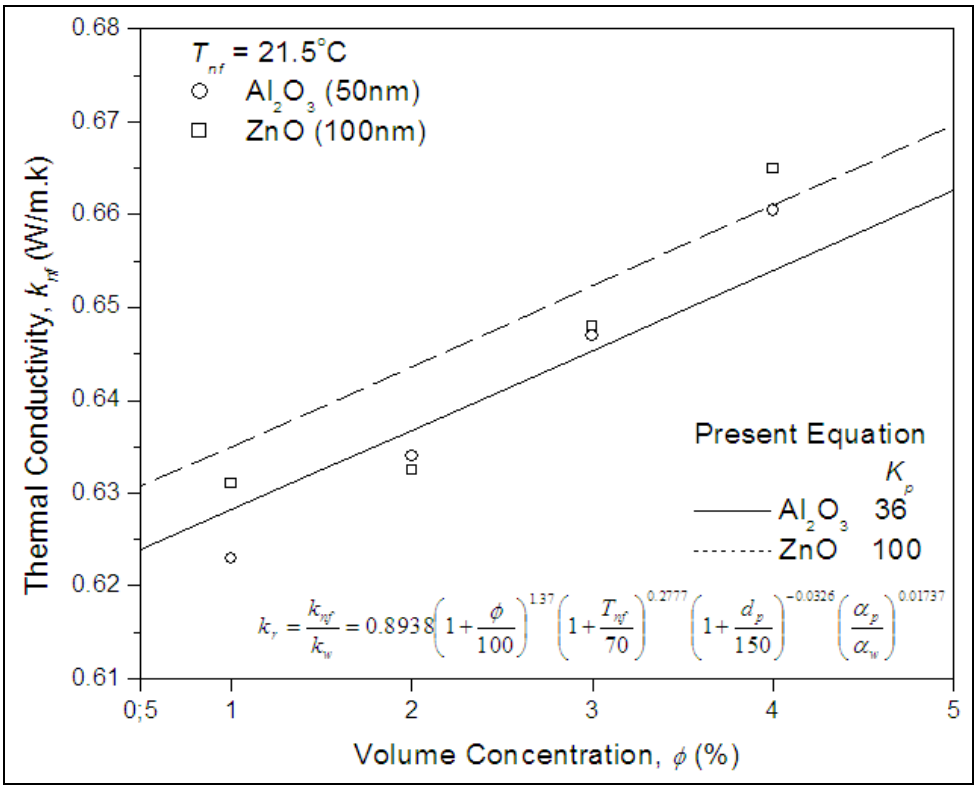


**Figure 4.1:** Comparison of Thermal Conductivity Correlation

### 4.2.2 Viscosity

Comparison of the measured viscosity of water based nanocoolants with the proposed correlation was shown as Figure 4.2. The figure shows $Al_2O_3$/water, ZnO/water and $TiO_2$/water nanocoolants for particle diameters of 50nm, 100nm and 150nm, respectively. The measured data gives the effect of different materials, particle size and volume concentration to the values of viscosity at ambient temperature of 21.5$^o$C. The viscosity estimated using the proposed equation is in a good agreement with the measured data for different nanocoolants tested.

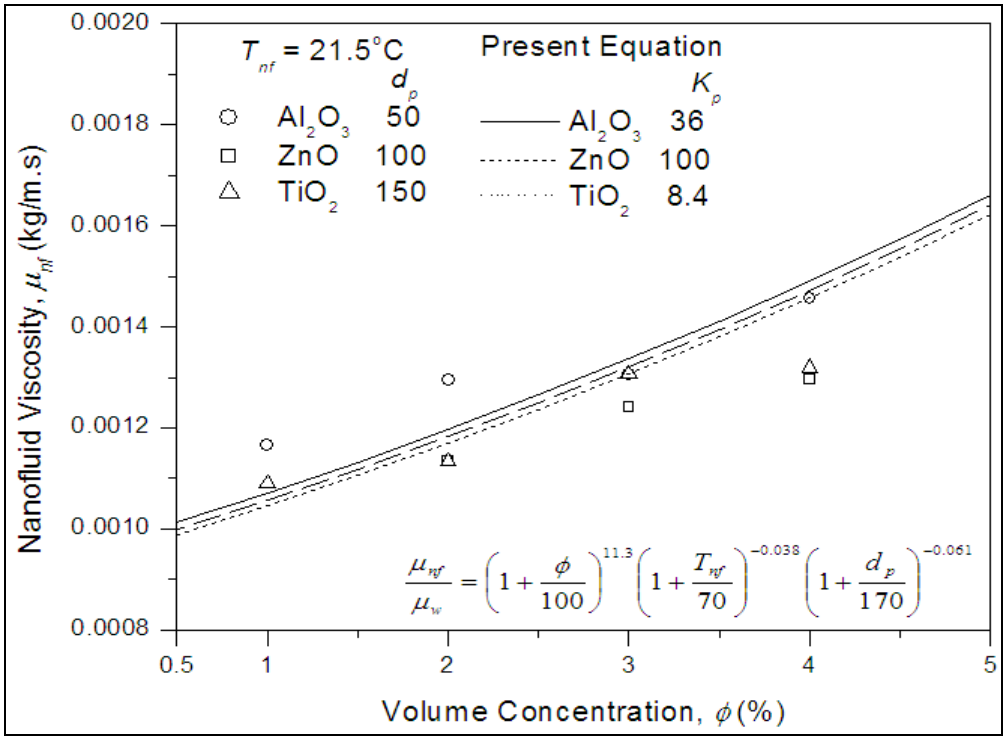


**Figure 4.2:** Comparison of Viscosity Correlation

## 4.3 SURFACE ROUGHNESS

The grinding process was carried out using the material of aluminium alloy (Al 6061) varying depth of cut. The grinding wheel used was silicon carbide. Then, the surface roughness of the grinded material was measured by using Mahr Perthometer. The material is divided into three parts which were initial, medium and final. The average value of the measurement was taken. The units for the surface dimensions are in micrometer (μm). The result for the single-pass and multi-pass grinding process using water based coolant as in (Table 4.1) and (Table 4.2) respectively (Jamilah, 2011). While the grinding process using zinc oxide nanocoolant was tabulated in (Table 4.3) and (Table 4.4) respectively.

The graph on Figure 4.4 shows the graph of surface roughness versus depth of cut for single-pass and multi-pass experiment using both $ZnO_2$ nanocoolant and also water based coolant. It is clearly shown that when the depth of cut increase the surface roughness also increase for all type of grinding. The surface roughness for

water based coolant higher compared to $ZnO_2$ nanocoolant. The multi-pass grinding process using $ZnO_2$ nanocoolant has the lowest surface roughness, while single-pass grinding process using water based coolant has the highest surface roughness. When the depth of cut increase, the force applied on the grinding surface also increase, this lead to the increase in heat transferred from the wheel to the material and cause the surface get rougher (Demir et al,. 2010).

Figure 4.3 (a) and (b) show the silicon carbide wheel surface after single-pass and multi-pass grinding process respectively. It is known as build-up-edge. The wheel condition after single-pass grinding has less coated aluminium compared than the wheel of multi-pass grinding. This coated appear on the wheel because aluminium tend to melt when more force and heat are transferred from the wheel. Aluminium is a not a hard material, so it easily melt on higher temperature and stick on the wheel. This cause the wheel becomes rougher and less sharp. The stone would grind the aluminum for a while, but particles would start getting embedded in the pores of the stone. And the next time the stone comes around, there's no grit exposed, only little bits of aluminum. So the aluminum on the piece rubs against the aluminum on the wheel, producing more heat, which produces more melting, and so on. The wheel condition influences the material surface. The wheel roughness is the reason for the material to become rougher.

The grinding process of water based coolant has higher surface roughness than zinc oxide nanocoolant grinding. This happen because the thermal conductivity of nanocoolant higher than water based coolant. The usage of nanocoolant as cutting fluid has reduced the amount of heat transferred from the wheel. This is because the nanocoolant has high thermal conductivity, refer (Table 2.4 - Incropera and DeWitt, 2001), due to that the wheel temperature also decreased, so the heat transferred from the wheel also will decrease. When the heats produced are less, the grinding process will be smoother and the surface also will be fine.

Nanocoolants are promising heat transfer fluids due to the high thermal conductivity enhancements (Heris et al., 2006). Heat transfer performance of

nanocoolant is significantly more dependent on temperature when compared to pure fluids (Kim et al., 2009). A study by (Ding et al., 2005) observed that the viscosity of nanocoolants decreased with increasing temperature. That means the nanocoolants can provide better fluid flow performance due to the higher shear rate at the wall, which results in low viscosity there. It can perform as a better lubricating fluid. The advanced heat transfer and tribological properties of these nanocoolants can provide better cooling and lubricating in the grinding process (Bin Shen, 2008).

**(a)**

**(b)**

**Figure 4.3:** Wheel Surface after Grinding, (a)Single-pass and (b)Multi-pass

**Table 4.1 :** Surface Roughness using Water Based Coolant (Single-pass)

| Depth of Cut (µm) | Surface Roughness (µm) | | | | | | | | | |
|---|---|---|---|---|---|---|---|---|---|---|
| | Initial | | | Medium | | | Final | | | Average |
| | 1 | 2 | 3 | 1 | 2 | 3 | 1 | 2 | 3 | |
| 5 | 2.47 | 1.15 | 1.57 | 3.19 | 1.62 | 5.31 | 1.71 | 1.42 | 1.27 | 2.19 |
| 7 | 2.89 | 2.6 | 2.83 | 2.34 | 3.16 | 2.22 | 0.70 | 2.45 | 0.85 | 2.22 |
| 9 | 3.84 | 2.47 | 2.18 | 1.07 | 1.9 | 1.46 | 3.56 | 1.28 | 3.11 | 2.32 |
| 11 | 2.19 | 2.14 | 1.27 | 3.72 | 2.48 | 1.55 | 2.62 | 3.00 | 3 | 2.43 |
| 13 | 3.16 | 3.04 | 3.52 | 3.35 | 2.76 | 1.40 | 1.94 | 1.95 | 1.95 | 2.56 |
| 15 | 3.10 | 3.53 | 2.33 | 2.12 | 2.97 | 2.21 | 2.51 | 2.31 | 2.46 | 2.61 |
| 17 | 3.51 | 4.71 | 3.42 | 1.79 | 1.40 | 3.27 | 3.06 | 1.48 | 2.27 | 2.77 |
| 19 | 3.85 | 3.01 | 3.84 | 3.31 | 3.40 | 3.05 | 2.42 | 1.99 | 1.65 | 2.94 |
| 21 | 3.77 | 4.05 | 3.60 | 1.92 | 3.32 | 3.56 | 2.23 | 3.66 | 1.97 | 3.12 |

Source : Jamilah Mustafha, 2011

**Table 4.2 :** Surface Roughness using Water Based Coolant (Multi-pass)

| Depth of Cut (µm) | Surface Roughness (µm) | | | | | | | | | |
|---|---|---|---|---|---|---|---|---|---|---|
| | Initial | | | Medium | | | Final | | | Average |
| | 1 | 2 | 3 | 1 | 2 | 3 | 1 | 2 | 3 | |
| 5 | 2.27 | 1.22 | 1.23 | 1.79 | 1.39 | 1.68 | 2.14 | 2.01 | 1.3 | 1.67 |
| 7 | 1.42 | 2.04 | 1.28 | 1.51 | 2.06 | 1.64 | 2.19 | 2.88 | 2.14 | 1.90 |
| 9 | 2.86 | 2.92 | 2.85 | 2.73 | 1.03 | 1.30 | 1.38 | 2.10 | 1.97 | 2.13 |
| 11 | 2.52 | 2.51 | 2.80 | 1.97 | 1.98 | 2.14 | 1.99 | 2.45 | 2.56 | 2.33 |
| 13 | 2.20 | 2.20 | 2.35 | 3.75 | 2.58 | 2.62 | 1.38 | 2.36 | 2.45 | 2.43 |
| 15 | 2.10 | 2.62 | 2.52 | 2.42 | 2.45 | 2.85 | 2.32 | 2.13 | 2.90 | 2.48 |
| 17 | 2.11 | 2.77 | 2.95 | 2.79 | 2.16 | 2.41 | 2.15 | 2.94 | 2.19 | 2.50 |
| 19 | 2.80 | 2.58 | 2.66 | 2.35 | 2.26 | 2.14 | 2.05 | 2.31 | 3.73 | 2.54 |
| 21 | 2.45 | 2.24 | 2.33 | 2.32 | 2.96 | 3.30 | 2.72 | 2.35 | 2.96 | 2.62 |

Source : Jamilah Mustafha, 2011

**Table 4.3 :** Surface Roughness using Zinc Oxide Nanocoolant (Single-pass)

| Depth of cut (µm) | Surface Roughness (µm) | | | |
|---|---|---|---|---|
| | **Initial** | **Medium** | **Final** | **Average** |
| **5** | 1.125 | 1.091 | 1.176 | 1.131 |
| **7** | 1.246 | 1.287 | 1.243 | 1.259 |
| **9** | 1.305 | 1.331 | 1.396 | 1.344 |
| **11** | 1.497 | 1.454 | 1.508 | 1.486 |
| **13** | 1.683 | 1.623 | 1.667 | 1.658 |
| **15** | 1.741 | 1.717 | 1.697 | 1.718 |
| **17** | 1.801 | 1.818 | 1.793 | 1.804 |
| **19** | 1.897 | 1.837 | 1.834 | 1.856 |
| **21** | 2.023 | 1.903 | 1.941 | 1.956 |

**Table 4.4 :** Surface Roughness using Zinc Oxide Nanocoolant (Multi-Pass)

| Depth of cut (µm) | Surface Roughness (µm) | | | |
|---|---|---|---|---|
| | **Initial** | **Medium** | **Final** | **Average** |
| **5** | 0.972 | 0.931 | 0.996 | 0.966 |
| **7** | 1.097 | 1.054 | 1.108 | 1.086 |
| **9** | 1.183 | 1.123 | 1.167 | 1.158 |
| **11** | 1.217 | 1.299 | 1.214 | 1.243 |
| **13** | 1.364 | 1.327 | 1.324 | 1.338 |
| **15** | 1.415 | 1.495 | 1.457 | 1.456 |
| **17** | 1.533 | 1.554 | 1.522 | 1.536 |
| **19** | 1.698 | 1.711 | 1.707 | 1.705 |
| **21** | 1.787 | 1.823 | 1.754 | 1.788 |

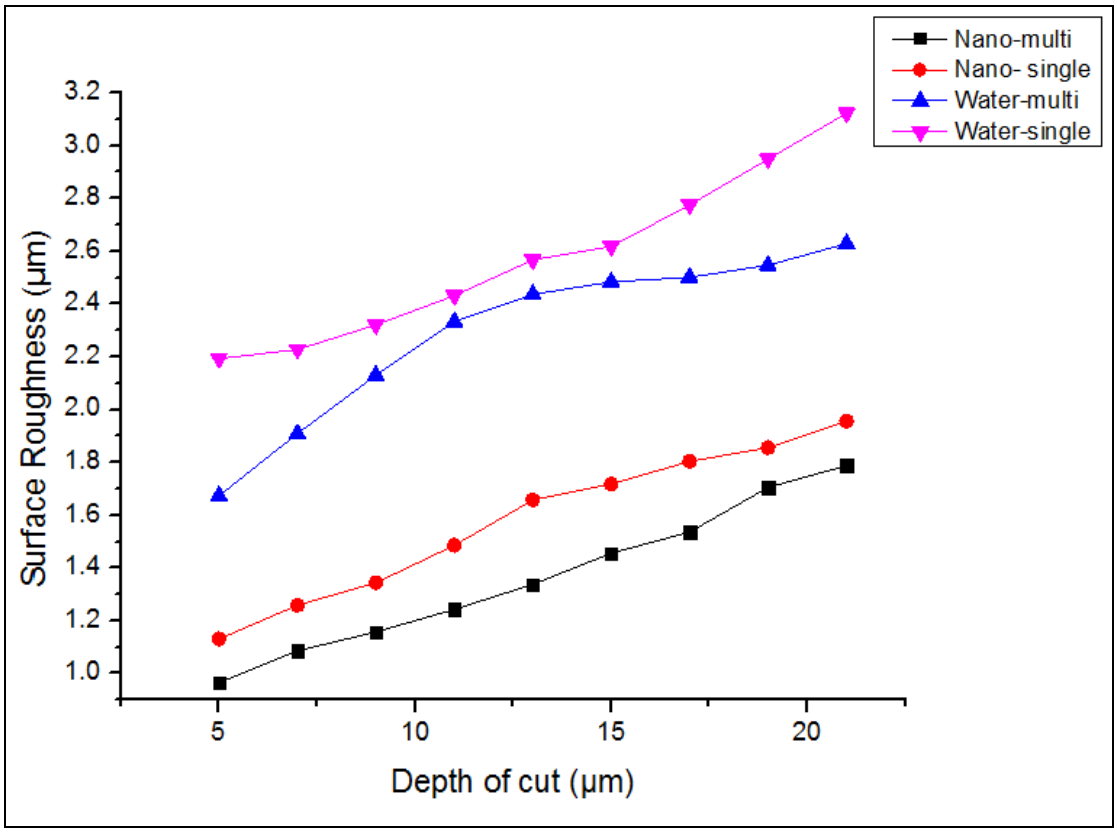


**Figure 4.4** : Surface Roughness versus Depth of Cut

Apart from the surface roughness measurement, the 2D microstructure of the grinded part of the material was observed. Figure 4.6 shows the observed 2D microstructure according to the depth of cut for single-pass and multi-pass grinding. The labeled Figure 4.5 (a), (b) and (c) microstructure are for multi-pass grinding while Figure 4.6 (d), (e) and (f) are for single-pass grinding. From the microstructure figure below, it is clearly shown the roughness of surface increase with the increasing depth of cut. The observed microstructure for multi-pass grinding with 5µm depth of cut shows the finest surface while the microstructure of single-pass with 21µm depth of cut shows the roughest surface. The microstructure looks very rough when the depth of cut increase because the friction between the wheel and material increases.

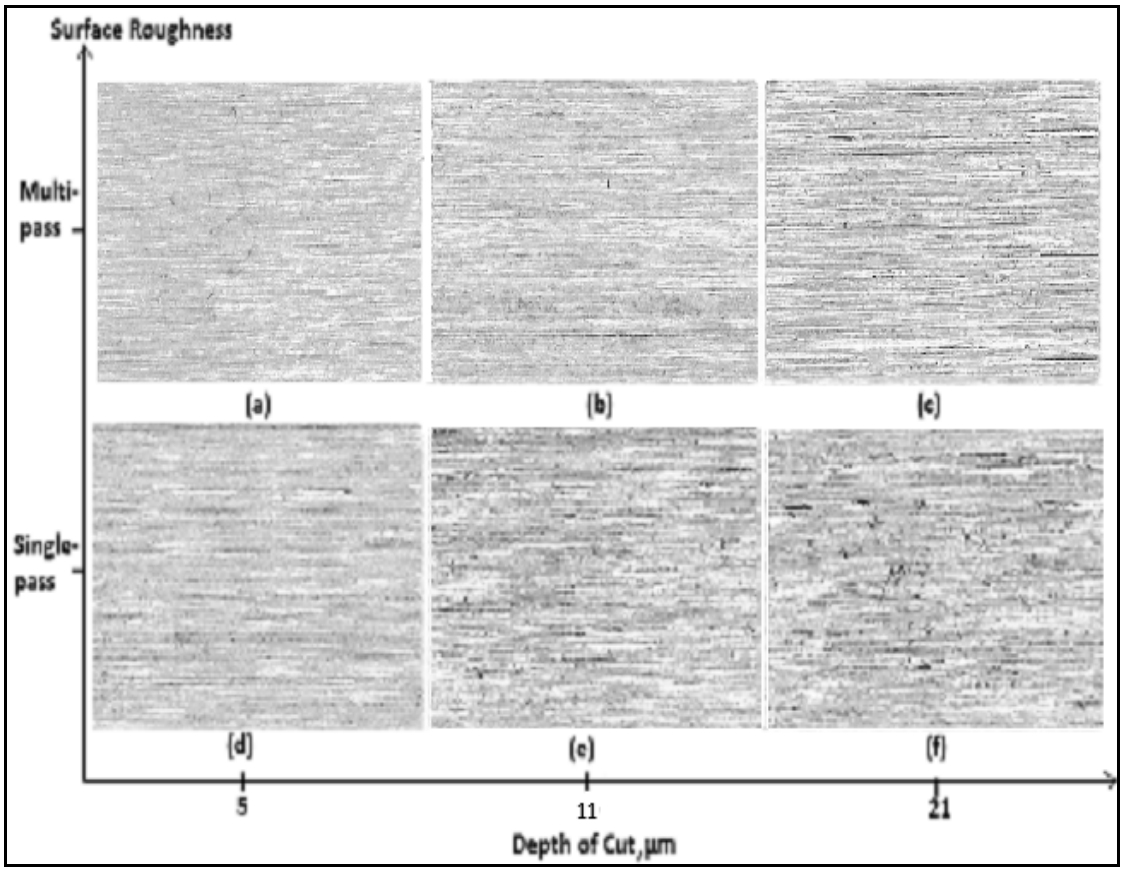


**Figure 4.5:** 2D Microstructure of Aluminium Alloy (6061)

## 4.4 WHEEL WEAR

The wheel wear for the each depth of cut for both single and multi-pass was estimated. The wheel diameter was measured using vernier caliper. The wheel diameter was measured before and after the experiment and the wheel wear was calculated. The wheel ratio can also be defined as wheel wear. The wheel ratio is the difference between the wheel diameter of initial and final.

Referring to the below result, it shows that the wheel wear for both single-pass and multi-pass were unchangeable. The wheel diameter after the experiment remains the same as before the experiment. This is because the depth of cut for each experiment is in small unit which was in micrometer (µm) and the changes of wheel diameter also might be very small. Since, vernier caliper was used for wheel

diameter measurement and the unit of vernier caliper was in millimeter (mm), the small changes in wheel diameter were unable to identify. Due to that, the wheel wear was neglected in this study.

**Table 4.5:** Wheel Ratio for Single-Pass Experiment

| **Depth of cut (µm)** | **Wheel Diameter (mm)** | | |
|---|---|---|---|
| | **Initial** | **Final** | **Wheel Ratio** |
| **5** | 164.42 | 164.42 | - |
| **7** | 164.36 | 164.36 | - |
| **9** | 164.27 | 164.27 | - |
| **11** | 164.17 | 164.17 | - |
| **13** | 164.06 | 164.06 | - |
| **15** | 163.92 | 163.92 | - |
| **17** | 163.77 | 163.77 | - |
| **19** | 163.59 | 163.59 | - |
| **21** | 163.39 | 163.39 | - |

**Table 4.6:** Wheel Ratio for Multi-Pass Experiment

| **Depth of cut (µm)** | **Wheel Diameter (mm)** | | |
|---|---|---|---|
| | **Initial** | **Final** | **Wheel Ratio** |
| **5** | 161.77 | 161.77 | - |
| **7** | 161.68 | 161.68 | - |
| **9** | 161.58 | 161.58 | - |
| **11** | 161.46 | 161.46 | - |
| **13** | 161.32 | 161.32 | - |
| **15** | 161.15 | 161.15 | - |
| **17** | 160.96 | 160.96 | - |
| **19** | 160.74 | 160.74 | - |
| **21** | 160.49 | 160.49 | - |

## 4.5 NEURAL NETWORK ANALYSIS

The obtained result of the experiment was trained and tested using Neural Network and the output of the trained result was tabulated as below for both single and multi-pass grinding process.

Based on the obtained result, the output was trained slightly similar with the target. The accuracy of the result can be defined with the r-square value. The r-square value of each trained result should be more than 0.85 to achieve the high accuracy. The r-square for graph actual versus output for single-pass was 0.96919 while for multi-pass was 0.96369. This means that the trained output graph for achieve the target result has high accuracy. Besides, the absolute error and absolute relative error value also was obtained for the trained result. This value was calculated based on the error percentage of the predicted output and obtained target. The error percentage for both single and multi-pass experiment shows a very small value, not more than 10%. The average roughness for obtained result and predicted output were tabulated in Table 4.8 (single-pass) and Table 4.11 (multi-pass). The average roughness values also have a very small error percentage.

The predicted roughness for various depth of cut, which were from depth of cut 23 µm to 49 µm were trained in neural network and were tabulated as in Table 4.9 and Table 4.12 for single-pass and multi-pass respectively. Next, the graph was plotted based on the predicted result of various depth of cut for both single and multi-pass using water based zinc oxide nanocoolant in Figure 4.8. The graph clearly shows that the surface roughness slightly increase with the increasing of depth of cut for predicted depth of cut (after the dotted line). But at one point, when the depth of cut was 37µm, the surface roughness values become constant. This happen because the plastic deformation occur.

### 4.5.1 Single-pass

**Table 4.7 :** Experimental Compare with Prediction Value(Single-pass)

| | Row | Depth of cut | Target | Output | Absolute Error | Absolute Relative Error |
|---|---|---|---|---|---|---|
| **TRN** | 0 | 5 | 1.131 | 1.22918 | 0.09818 | 8.68038 |
| **TRN** | 1 | 7 | 1.259 | 1.26663 | 0.00763 | 0.6062 |
| **TRN** | 2 | 9 | 1.344 | 1.34472 | 0.00072 | 0.05349 |
| **TRN** | 3 | 11 | 1.486 | 1.46785 | 0.01815 | 1.22168 |
| **TRN** | 4 | 13 | 1.658 | 1.60225 | 0.05575 | 3.36226 |
| **TRN** | 5 | 15 | 1.718 | 1.71744 | 0.00056 | 0.03246 |
| **VLD** | 6 | 17 | 1.804 | 1.80501 | 0.00101 | 0.05596 |
| **TRN** | 7 | 19 | 1.856 | 1.86336 | 0.00736 | 0.39675 |
| **TST** | 8 | 21 | 1.956 | 1.89724 | 0.05876 | 3.0042 |
| **Correlation :** | | 0.9913 | | **R-squared :** | | 0.96919 |

**Table 4.8 :** Summary of Training (Single-pass)

| | Target | Output | Absolute Error | Absolute Relative Error |
|---|---|---|---|---|
| **Mean:** | 1.65643 | 1.64238 | 0.01883 | 0.01073 |
| **Std Dev:** | 0.24222 | 0.23215 | 0.02448 | 0.01352 |
| **Min:** | 1.259 | 1.26663 | 0.00056 | 0.00033 |
| **Max:** | 1.956 | 1.89724 | 0.05876 | 0.03362 |

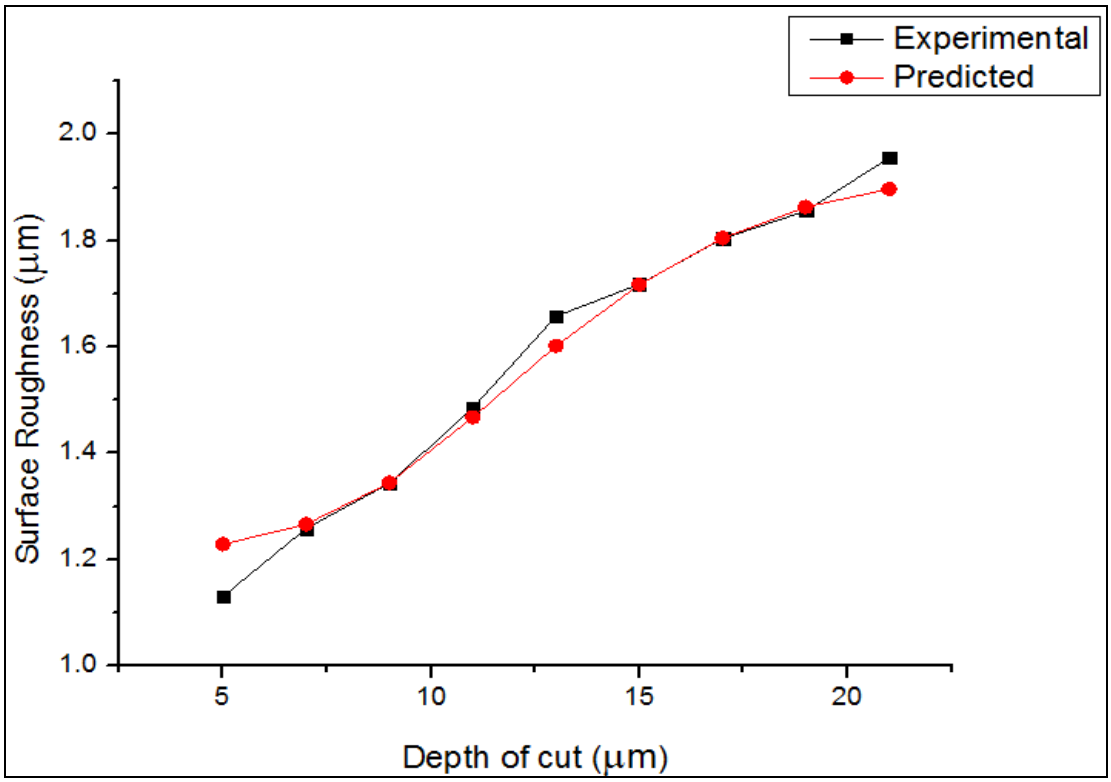


**Figure 4.6 :** Graph Experimental Compare with Prediction Value (Single-pass)

**Table 4.9 :** Prediction of various depth of cut (Single-pass)

| Depth of cut (µm) | Surface Roughness (µm) |
|---|---|
| **23** | 1.91531 |
| **25** | 1.92475 |
| **27** | 1.92975 |
| **29** | 1.93245 |
| **31** | 1.93395 |
| **33** | 1.93478 |
| **35** | 1.93526 |
| **37** | 1.93553 |
| **39** | 1.93568 |
| **41** | 1.93577 |
| **43** | 1.93582 |
| **45** | 1.93585 |
| **47** | 1.93586 |
| **49** | 1.93587 |

### 4.5.2 Multi-pass

**Table 4.10 :** Experimental Compare with Prediction Value (Multi-pass)

| | Row | Depth of cut | Target | Output | Absolute Error | Absolute Relative Error |
|---|---|---|---|---|---|---|
| **TRN** | 0 | 5 | 0.966 | 1.04966 | 0.08366 | 8.66057 |
| **TRN** | 1 | 7 | 1.086 | 1.08076 | 0.00524 | 0.48263 |
| **TRN** | 2 | 9 | 1.158 | 1.13524 | 0.02276 | 1.96526 |
| **VLD** | 3 | 11 | 1.243 | 1.2215 | 0.0215 | 1.7295 |
| **TST** | 4 | 13 | 1.338 | 1.33549 | 0.00251 | 0.18739 |
| **TRN** | 5 | 15 | 1.456 | 1.46383 | 0.00783 | 0.53756 |
| **TRN** | 6 | 17 | 1.536 | 1.58094 | 0.04494 | 2.92596 |
| **TRN** | 7 | 19 | 1.705 | 1.66109 | 0.04391 | 2.57533 |
| **TRN** | 8 | 21 | 1.788 | 1.70634 | 0.08166 | 4.567 |
| **Correlation :** | | 0.98863 | | **R-squared :** | | 0.96369 |

**Table 4.11 :** Summary of Training (Multi-pass)

| | Target | Output | Absolute Error | Absolute Relative Error |
|---|---|---|---|---|
| **Mean:** | 1.355 | 1.35614 | 0.03784 | 0.02939 |
| **Std Dev:** | 0.24883 | 0.22234 | 0.03097 | 0.02703 |
| **Min:** | 0.966 | 1.04966 | 0.00251 | 0.00187 |
| **Max:** | 1.788 | 1.70634 | 0.08366 | 0.08661 |

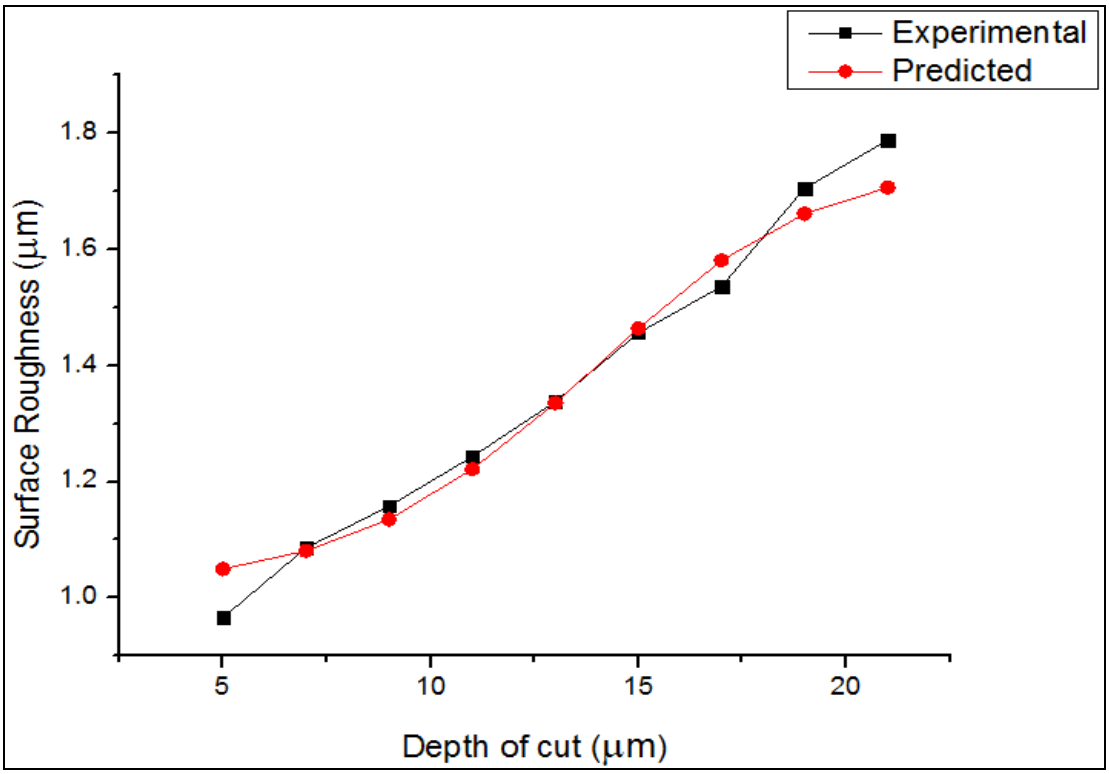


**Figure 4.7 :** Graph Experimental Compare with Prediction Value (Multi-pass)

**Table 4.12 :** Prediction of various depth of cut (Multi-pass)

| Depth of cut (µm) | Surface Roughness (µm) |
|---|---|
| 23 | 1.73041 |
| 25 | 1.74338 |
| 27 | 1.75064 |
| 29 | 1.75484 |
| 31 | 1.75736 |
| 33 | 1.75889 |
| 35 | 1.75984 |
| 37 | 1.76043 |
| 39 | 1.76081 |
| 41 | 1.76104 |
| 43 | 1.76119 |
| 45 | 1.76129 |
| 47 | 1.76135 |
| 49 | 1.76138 |

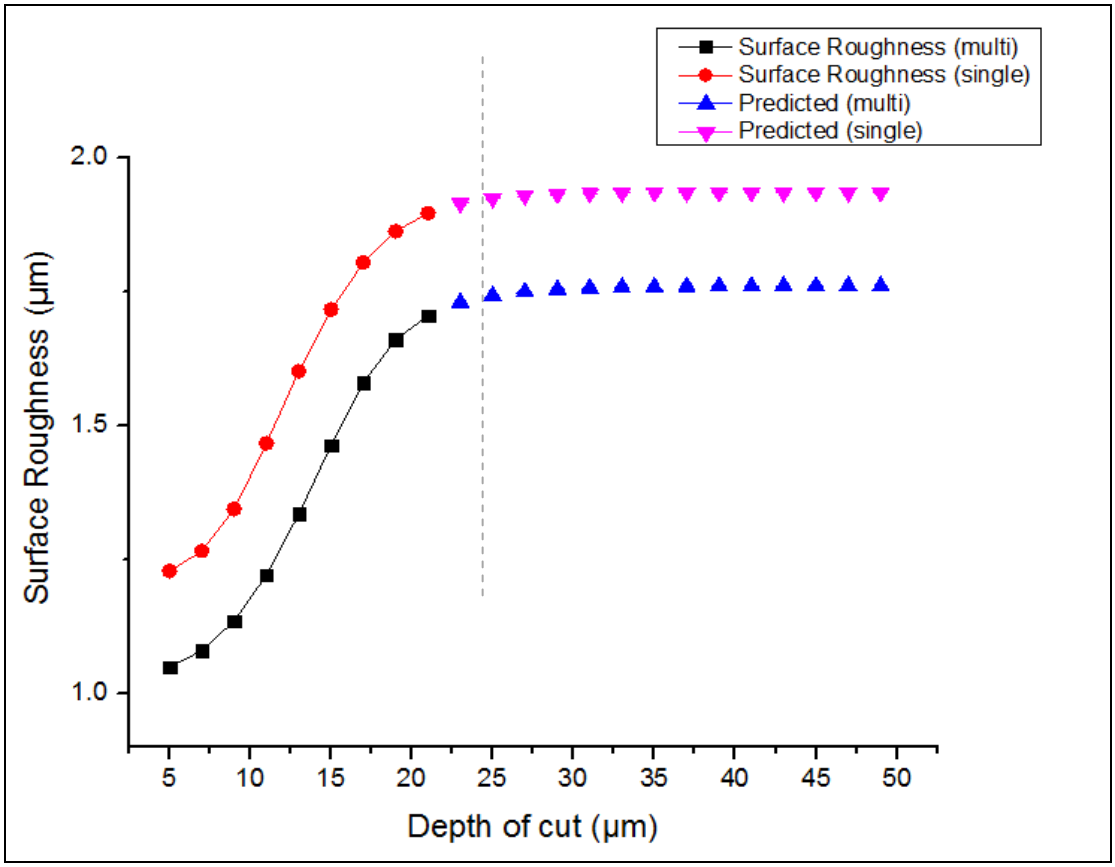


**Figure 4.8 :** Graph Prediction of Various Depth of Cut

# CHAPTER 5

# CONCLUSION

## 5.1 INTRODUCTION

This chapter mainly discuss about the conclusions that can be derived from this experiment. Besides that, it also suggests some future recommendations for the purpose of further studies in the field of manufacturing.

## 5.2 CONCLUSION

The surface roughness and wheel wear between the single-pass and multi-pass grinding process using water based coolant and zinc oxide nanocoolant were studied along this project. For the outcome of this project, the surface roughness increases with the increasing of depth of cut. Besides the result obtained for zinc oxide nanocoolant experiment as cutting fluid was 48.4 % much more better than water based coolant. Wheel wear for nanocoolant was better than water based coolant. But since there are no changes in the wheel ratio for zinc oxide nanocoolant, the wheel wear was neglected for this study. The usage of nanocoolant lead to the decrease in the surface roughness and also the wheel wear. The optimum depth of cut for this project was 5µm for both single and multi-pass grinding. The advanced heat transfer and tribological properties of these nanocoolants can provide better cooling and lubricating in the grinding process. The future prediction of various depth of cut

was analyzed using Artificial Neural Network (ANN). The surface roughness becomes constant when the depth of cut was 37 µm. As overall conclusion, the purpose of this project to investigate the type of surface roughness and wear was achieved. The second objective to develop the prediction model with the usage of zinc oxide nanocoolant was attained in this study.

## 5.3 FUTURE RECOMMENDATIONS

Recently, engineering applications in machining process are rapidly developing. Grinding is recognized as one of the most environmentally unfriendly manufacturing processes. Since cutting fluids are a critical factor in controlling undesirable effects of elevated temperatures, thermal damage, and dimensional inaccuracies in grinding process, more studies should be carried out as below:

a) Experiments are to be conducted with the usage of different type of nanocoolant and various concentrations.
b) Experiments also can be carried at different particle sizes of nanocoolant and investigate the heat transfer coefficients.
c) Use the different type and various size of conventional abrasive grinding wheel for the grinding process.

## REFERENCES

[1] V. Songmene, R. Khettabi, I. Zaghbani, J. Kouam, and A. Djebara, 2009, "Machining and Machinability of Aluminum Alloys", Theory and Applications.

[2] Xiang-Qi Wang, Arun S. Mujumdar, 2006, "Heat transfer characteristics of nanofluids", International Journal of Thermal Sciences , vol 46, pg 1-19.

[3] Bin Shen, 2008, "Minimum Quantity Lubrication Grinding Using Nanofluids".

[4] Alexius Anak An'yan, 2008, "Effect Of Grinding Process Parameters On Grinding Force Of Aluminium Alloys (Aa6061-t6)".

[5] Rusydah, 2008, "An Experimental Study Of Impact Of Surface Grinding Parameters

[6] Aguiar, P.R.; Bianchi, E. C. & Oliveira, J. F. G. (2008); A method for burning Detection in grinding process using acoustic emission and effective electrical power signal, *CIRP Journal of Manufacturing Systems, 31, 2002, 253-257, Paris.*

[7] Incropera, F.P. and DeWitt, D.P., 2001, Fundamentals of Heat and Mass Transfer, 5th Edition, Wiley.

[8] Chris Pfeifer, 2007, "Predicting the Grinding Process", Friction and Wear of Materials, Rensselaer Published.

[9] Khettabi, R., Songmene, V. and Masounave J. (2010 b). Influence of machining processes on particles emission, *49th Annual Conference of Metallurgists of CIM*, 4- 6 Oct. 2010,Vancouver, BC, Canada, pp. 277-288.

[10] Y. W. Tham, M. W. Fu, Q. X. Pei, and K. B. Lim, 2007, "Microstructure and Properties of Al-6061 Alloy by Equal Channel Angular Extrusion for 16 Passes", *Materials and Manufacturing Processes*, vol 22, page 819–824.

[11] Eastman, J. A., Choi, S. U. S., Li, S., Yu, W., and Thompson, L. J., 2001, "Anomalously Increased Effective Thermal Conductivities of Ethylene Glycol-Based Nanofluids Containing Copper Nanoparticles," Vol: 78(6), pp. 718-720.

[12] Yu, W., France, D. M., Routbort, J. L., and Choi, S. U. S., 2008, "Review and Comparison of Nanofluid Thermal Conductivity and Heat Transfer Enhancements," Heat Transfer Eng., 29(5), pp. 432-460.

[13] Heris, S. Z., Etemad, S., and Esfahany, M. N., 2006, "Experimental Investigation of Oxide Nanofluids Laminar Flow Convective Heat Transfer,"Heat Mass 33.

[14] Kim, D., Kwon, Y., Cho, Y., Li, C., Cheong, S., Hwang, Y., Lee, J., Hong, D., and Moon, S., 2009, "Convective Heat Transfer Characteristics of Nanofluids under Laminar and Turbulent Flow Conditions," Current Applied Physics, pp. 119- 123.

[15] Romano, J. M., Parker, J. C., and Ford, Q. B., 1997, "Application Opportunities for Nanoparticles Made from the Condensation of Physical Vapors,", pp. 12-13.

[16] Spanu, C., and Marinescu, I., 2002, Effectiveness of ELID Grinding and Polishing. International Manufacturing Conference IMTS: Chicago.

[17] Kalpakjian, S., *Manufacturing Engineering and Technology*, 4th Ed, Addisson-Wesley , New York, 2001.

[18] Erik J. Salisbury, K. Vinod Domala, Kee S. Moon, Michele Miller, John W.Sutherland, “A Three-Dimensional Model for the Surface Texture in Surface Grinding”, Transactions of the ASME, vol:123

[19] Hoshi, M., Omotani, T., and Nagashima, A., 1981, “Transient method to measure the thermal conductivity of high-temperature melts using a liquid-metal probe,” Review of Scientific Instruments, vol. 52, no. 5, pp. 755-758.

[20] DeGroot, J.J, J. Kestin, and H. Sookiazian, 1974, “Instrument to measure the Thermal conductivity of gases,” Physica, vol. 75, pp. 454-482.

[21] Nagasaka, Y, and Nagashima, A., 1981, “Absolute measurement of the thermal conductivity of electrically conducting liquids by transient hot-wire method”, J Phys E Sci Instrum, 1981, vol. 14, pp. 1435-1440.

[22] Stefan Feistrizer, Klaus Uldier, 2006, Diamond Coated Cutting Tools for Machining, International Journal of Refractory Metal, Vol24, 354-359

[23] Y. Ding, H. Alias, D. Wen, R.A. Williams, Heat transfer of aqueous suspensions of carbon nanotubes (CNT nanofluids), International Journal of Heat and Mass Transfer 49 (1–2) (2005) 240–250.